İSTANBUL TECHNICAL UNIVERSITY ★ INSTITUTE OF SCIENCE AND TECHNOLOGY

IN SITU SYNTHESIS OF OIL BASED POLYMER COMPOSITES CONTAINING SILVER NANOPARTICLES

Ph.D. Thesis by
Osman EKSİK

Department : Chemical Engineering

Programme : Chemical Engineering

JUNE 2009

İSTANBUL TECHNICAL UNIVERSITY ★ INSTITUTE OF SCIENCE AND TECHNOLOGY

IN SITU SYNTHESIS OF OIL BASED POLYMER COMPOSITES CONTAINING SILVER NANOPARTICLES

Ph.D. Thesis by
Osman EKSİK
(506002104)

Date of submission : 02 February 2009
Date of defence examination: 19 June 2009

Supervisor (Chairman) : Prof. Dr. A. Tuncer ERCİYES (ITU)
Members of the Examining Committee : Prof. Dr. Nuran DEVECİ (ITU)
Prof. Dr. Yusuf YAĞCI (ITU)
Prof. Dr. Ahmet KAŞGÖZ (IU)
Prof. Dr. Mehmet Ali GÜRKAYNAK (IU)

JUNE 2009

İSTANBUL TEKNİK ÜNİVERSİTESİ ★ FEN BİLİMLERİ ENSTİTÜSÜ

NANO GÜMÜŞ PARTİKÜLLERİ İÇEREN YAĞ BAZLI POLİMER KOMPOZİTLERİN SENTEZİ

DOKTORA TEZİ

Osman EKSİK
(506002104)

Tezin Enstitüye Verildiği Tarih : 02 Şubat 2009
Tezin Savunulduğu Tarih : 19 Haziran 2009

Tez Danışmanı : Prof. Dr. A. Tuncer ERCİYES (İTÜ)
Diğer Jüri Üyeleri : Prof. Dr. Nuran DEVECİ (İTÜ)
Prof. Dr. Yusuf YAĞCI (İTÜ)
Prof. Dr. Ahmet KAŞGÖZ (İÜ)
Prof. Dr. Mehmet Ali GÜRKAYNAK (İÜ)

HAZİRAN 2009

FOREWORD

First, I would like to thank my advisor, Professor Tuncer Erciyes, for his encouragement, guidance, and his insightful view of the polymer field. Not only did he open my eye to the fascinating world of polymer chemistry, more importantly, he also educated me on how to appreciate the beauty of polymer science and how to develop the focus on scientific research. Without his knowledge and expertise, I would have never been able to accomplish the work of my graduate research.

I would also like to express my gratitude to Professor, Yusuf Yagcı for serving on my committee and making valuable suggestions.

I would like to thank to Assc. Prof. Dr. Seyhun Solakoğlu from Çapa Medical Faculty of Istanbul University for conducting our TEM observations.

I wish to thank to my current laboratory colleagues for all their help and guidance. In particular, Dr. M. Atilla Taşdelen, Res. Asst. Neslihan Alemdar and Esra Engin, with all of you, it has really been a great pleasure.

Finally, I would like to dedicate my thesis to my dearest father, mother, brothers, sisters and nephews, their love and support over the years makes my life more meaningful and enjoyable.

This work is supported by ITU Institute of Science and Technology.

June 2009

Osman EKSİK

Chemical Engineering M.Sc.

TABLE OF CONTENTS

Page

ABBREVIATIONS

TEM	: Transmission Electron Microscopy
SEM	: Scanning Electron Microscopy
AFM	**:** Atomic Force Microscopy
FT-IR	: Infrared Spectrophotometer
UV	: Ultra Violet
GPC	: Gel Permeation Chromatography
TGA	: Thermogravimetric Analysis
DMA	: Dynamic Mechanical Analysis
PANI	: Polyaniline
PVA	: Poly(vinyl alcohol)
PI	**:** Polyimide
PAA	: poly(acrylic acid)
UAN	: Urethane Acrylate Nwsoenionomer
AIBN	: 2,2-Azoisobutyronitrile
DMPA	: 2,2-Dimethoxy-2-phenyl acetophenone
THF	: Tetrahydrofuran
TDI	: Toluene Diisocyanate
HEMA	: 2-Hydroxyethyl Methacrylate
DGEBA	: Diglycidyl Ether of Bisphenol
PVP	: Poly(vinylpyrrolidone)
BSPP	: Bis(p-sulfonatophenyl) phenylphosphine dihydrate dipotassium salt
TOAB	: Tetraoctylammonium Bromide
AOT	: Sodium di-2-ethylhexylsulfosuccinate
OBPC	: Oil Based Polymer Composite
ESO	: Epoxidized Soybean Oil
VOCs	: Volatile Organic Compounds
PVD	: Physical Vapor Deposition
CVD	: Chemical Vapor Deposition
SMAD	: Solvated Metal Atom Dispersion
SERS	: Surface Enhanced Raman Spectroscopy
ASTM	: American Standard Test Method
ACRES	: Affordable Composites from Renewable Sources
EB	: Electron Beam
PI	: Photoinitiator
PEO	: Poly(ethylene oxide)
FA	: Fatty Acid
DNA	: Deoksiribonükleik asit

LIST OF TABLES

LIST OF FIGURES

LIST OF SYMBOLS

λ	**:** Wavelength
h*υ*	**:** Radiation
R·	**:** Radical
nm	**:** Nanometer
µm	**:** Micrometer
T_g	**:** Glass-transition temperature
K_{IC}	**:** Stress intensity factor
G_{IC}	**:** Fracture energies

IN SITU SYNTHESIS OF OIL BASED POLYMER COMPOSITES CONTAINING SILVER NANOPARTICLES

SUMMARY

Polymer/metal nanocomposites have attracted strong attention because of the combination of both the properties of the inorganic nanoparticles such as optical, antimicrobial, electrical, or mechanical and those of the polymer as processability, solubility, and chemical resistance. Polymer/metal nanocomposites can be obtained by two different approaches, namely, *ex situ* and *in situ* techniques. In the *ex situ* approach, polymerization of monomers and formation of metal nanoparticles were separately performed, and then they were mechanically mixed to form nanocomposites. In this approach, a wide size distribution of metal nanoparticles and poor dispersion in the polymer matrix were usually observed. In the *in situ* methods, metal particles are generated inside a polymer matrix by decomposition (e.g., thermolysis, photolysis, etc.) or chemical reduction of a metallic precursor dissolved into the polymer. Commonly employed *in situ* method is the dispersion process, in which the solutions of the metal precursor and the protective polymer are combined, and the reduction is subsequently performed in solution.

In this thesis, we describe two strategies for the in situ synthesis of triglyceride oil based polymer/silver nanocomposite in which silver nanoparticles were formed by electron transfer reaction. Polymer/silver nanocomposites were prepared by thermally induced and photochemically induced polymerization processes.

In the first strategy, using electron transfer reaction and free radical polymerization processes a series of triglyceride oil based polymer/silver nanocomposites were successfully prepared. The whole process was divided into two simultaneous stages; (i) copolymerization of macromonomers obtained from partial glycerides with styrene and (ii) the reduction of silver nitrate to metallic silver nano particles with radicals stemming from the thermolysis of 2,2'-azoisobutyronitrile. In the second strategy, *in situ* synthesis of oil based polymer/silver nanocomposites was prepared by using photoinduced free radical polymerization processes in which silver nanoparticles were formed by electron transfer reaction. An oil based macromonomer was prepared and then copolymerized with styrene in the presence of silver nitrate. Copolymerization was started with free radicals formed by photolysis of 2,2-dimethoxy-2-phenyl acetophenone and simultaneously silver nitrate was reduced to metallic silver in nano-sized by electron transfer reaction.

In this study, the composites obtained in thermally induced and photochemically induced polymerization processeses contain homogenously distributed silver nanoparticles in the network without macroscopic agglomeration and exhibit good film as organic coating with antibacterial properties. It should also be emphasized

that the importance of this study is closely related to the components of the network structure. The precursor triglyceride oil is obtained from renewable agricultural sources. Recently, the use of renewable sources in the preparation of various industrial materials has been revitalized because of the environmental concerns.

NANO GÜMÜŞ PARTİKÜLLERİ İÇEREN YAĞ BAZLI POLİMER KOMPOZİTLERİN SENTEZİ

ÖZET

Polimer/metal nano kompozit malzemeler, kimyasallara karşı gösterdiği direnç, kolay işlenebilirlik ve sahip oldukları üstün optik, antibakteriyel, elektriksel ve mekaniksel özellikler nedeniyle, gerek endüstriyel gerekse akademik çalışmalarda gittikçe artan bir öneme sahip olmaktadır. Polimer/metal nano kompozitler iki değişik yaklaşımla elde edilir. Bunlar, ex situ ve in situ yöntemleridir. *Ex situ* yönteminde, monomerlerin polimerizasyonu ve metal nano partiküllerin sentezi ayrı ayrı yapıldıktan sonra, mekaniksel olarak karıştırılır. Bu metodla elde edilen polimer nano kompozitlerde, metal nano partiküllerin boyutu büyük ve polimer matris içinde dağılımı çok zayıftır. *In situ* teknigiyle sentezlenen polimer nano kpompozitlerde ise metal nano partiküller polimer matris içinde bozunma (termal, fotokimyasal) veya kimyasal redüksiyon işlemine maruz bırakılarak elde edilir. Metal nano partiküllerin boyutu küçük ve bu partiküllerin polimer matris içinde dağılımı homojendir. Bu nedenle polimer nano kompozitlerin sentezinde *in situ* tekniğinin kullanılması yaygınlaşmıştır. Bu yöntemde çözelti formundaki metal öncü yapılar, koruyucu polymer içinde çözündürülür ve bunu takip eden redüksiyon işlemi ile polimer matrisi içinde nano partiküllerin oluşumu sağlanır.

Bu tezde, farklı iki polimerizasyon stratejisi izlenerek, in situ yöntemi ile yağ bazlı polimer gümüş nano kompozitler sentezlenmiştir. Termal ve fotokimyasal polimerizasyon prosesleri kulanılarak polimer sentezlenirken eş zamanlı olarak elektron transfer reaksiyonu ile gümüş partikülleri metalik nano partiküllere dönüştürülmüştür.

İlk strateji kullanılarak, termal olarak başlatılan serbest radikal polimerizasyonu ve electron transfer reaksiyonu ile polimer nano kompozitler başarıyla sentezlenmiştir. Buradaki bütün proses iki kısımdan oluşmaktadır; (i) Kısmi gliseridlerden elde edilen yağ bazlı macromonomer ile stirenin kopolimerizasyonu (ii) 2,2'-azoizobutironitril' in termal bozunmasıyla ortaya çıkan serbest radikallerin gümüş nitratı metalik nano partiküllere dönüştürmesi. İkinci strateji kullanılarak, polimer nano kompozit sentezlenmesi ve gümüş nano partiküllerin oluşumu serbest radikal fotopolimerizasyonu ve elektron transfer reaksiyonu ile gerçekleşmiştir. Hazırlanan yağ bazlı makromonomer gümüş nitrat varlığında stiren monomeri ile ultraviolet ışığına maruz bırakılarak kopolimerizasyon reaksiyonuna sokulmuştur. Bu reaksiyonda, 2,2-dimetoksi asetofenon foto başlatıcısı fotoliz yoluyla parçalanıp serbest radikal polimerizasyonunu başlatırken, aynı anda elektron transfer reaksiyonu ile gümüş nitrat metalik nano partiküllere dönüşmesi gerçekleşmektedir.

Bu çalışmada, termal ve fotokimyasal serbest radikal polimerizasyonu ile elde edilen polimer nano kompozitlerde, gümüş partiküllerinin polimer matris içerisinde aglomere olmadan homojen olarak dağıldığı görülmüştür. Ayrıca elde edilen nano kompozit ürünlerin film özelliklerinin konvensiyonel yolla elde edilen filmlere göre daha iyi olduğu ve antibakteriyel özellik gösterdiği saptanmıştır. Bu çalışmada asıl göz önünde bulundurulması gereken nokta ise elde edilen nano kompozit ürünlerin yapısıdır. Polimer nanokompozit ürünlerinin sentezinde başlangıç maddesi olarak yenilenebilir bir kaynak olan bitkisel yağın kullanılması, çevresel endişelerin arttığı bu günlerde, çalışmanın endüstriyel alanda gittikçe artan bir öneme sahip olacağını göstermektedir.

1. INTRODUCTION

Polymer/inorganic nanoparticle composites have attracted much interest during the past decade due to their unique size dependent chemical and physical properties [1-6]. Polymer nanocomposite materials have many uses in aerospace, automotive, marine, infrastructure, military, sports and industrial fields. Dispersion of very small metal particles in polymeric matrixes has proved to be an effective and low-cost method to improve the performance of the already existing polymer material properties such as mechanical properties, elasticity, transparency or specific absorption of light, optical properties, electrical conductivity, and, antimicrobial effects [7-13]. As a result of these properties, they have become an attractive alternative to materials such as steel, aluminum, and concrete.

Several approaches have been used to prepare polymer/metal nanocomposites. As a conventional method, polymerization of monomers and formation of metal nanoparticles were separately performed, and then they were mechanically mixed to form composites [14]. However, it is extremely difficult to disperse nanoparticles homogeneously into the polymer matrix by *ex situ* methods because of the easy agglomeration of nanoparticles [15]. A disturbing factor in such a filled polymer system has non-uniformity of composite properties owing to poor dispersion of the particles in the polymer. Surface modification of the filler with suitable coupling agent is often recommended to enhance filler dispersion as well as to prevent filler agglomeration [16]. Therefore, the convenient and effective ways of preparing nanoparticles in polymer materials are still in strong demand. For this purpose various methods were used to produce metal nanoparticles within a polymeric matrix. Most of them are based on *in situ* reactions, that is, the particles are generated from the respective metal precursors in the presence of the matrix polymer. The options for *in situ* formation of nanoparticles range from chemical reductions, photoreductions and thermal decompositions, to vapor deposition [17-20]. Commonly employed method is the dispersion process, in which the solutions

of the metal precursor and the protective polymer are combined, and the reduction is subsequently performed in solution. Another method concerns immersion process where the solid polymeric material is placed into a solution containing the metal precursor. Uptake of the metal precursor proceeds by diffusion into the swollen polymeric matrix. After drying, the reduction is performed within the solid sample. Alternatively, the combined solutions containing the metal precursor and the polymer are deposited onto a substrate, and the reduction to the metal colloids is performed within the thin solid film after removal of the solvent [21,22]. Additionally, a number of polymers, containing nano particles, prepared by reducing the polymer–metal chelates were reported. Typical examples include polyaniline (PANI)/Au, poly(vinyl alcohol) (PVA)/Ag, polyimide (PI)/Ag, and poly(acrylic acid) (PAA)/Cu–composites [4,23,24]. However, both polymer and metal nanoparticle formation simultaneously in the same reaction media has not been often employed. Kim et al. reported simultaneous synthesis of silver nanoparticles and the polymer film constituting the nanocomposite film through an *in situ* electron transfer reaction and the copolymerization of styrene with amphiphilic urethane acrylate nonionomer (UAN), which contains hydrophobic poly(propylene oxide) segments and hydrophilic poly(ethylene oxide) segments along the same backbone [25].

The selection of the polymeric matrix for the polymer/inorganic hybrid materials is crucial for the optimization of the systems. Frequently, the polymers are not only employed as protective polymers, but also used as a dispersing and stabilizing media for the metal nanoparticles. Amphiphilic block copolymers seemed to be remarkably suitable materials for this purpose. In addition to the good dispersion effect, the size of the nanoparticles dispersed within this matrix can be controlled by changing the block lengths of the hydrophobic and hydrophilic chains in the amphiphilic block copolymers [7]**.** However, amphiphilic block copolymers are very expensive materials and can only be obtained using extremely complicated synthetic processes. In the present study, a novel strategy was applied to synthesize nanocomposites from triglyceride oil based polymer exhibiting an amphiphilic characteristic to facilitate the formation of nanoparticles. Triglyceride oils have been widely used in the preparation of polymers not only because of the environmental and energytical issues, but also for improving the end-product properties. In this dissertation, sunflower oil was converted to partial glycerides and then combined with suitable

vinyl monomer to obtain macromonomer. The structure of the macromonomer was confirmed by Fourier transform infrared spectroscopy (FT-IR) analysis. The oil based vinyl macromonomer thus obtained was copolymerized with styrene. Using electron transfer, free radical polymerization and photoinduced free radical polymerization processes a series of triglyceride oil based polymer/silver nanocomposites were successfully prepared. The whole process was divided into two simultaneous stages; (i) copolymerization of macromonomers obtained from partial glycerides with styrene and (ii) the reduction of silver nitrate to metallic silver nano particles with radicals stemming from the thermolysis of 2,2'-azoisobutyronitrile (AIBN) or photolysis of 2,2- dimethoxy-2-phenyl acetophenone (DMPA). Metal ions in the polymer matrix are reduced thermally, or photochemically by UV/γ - irradiation. The amount of initiator influenced the size of silver nanoparticles formed within the polymer films. Nanocomposite films were characterized by using transmission electron microscopy (TEM), thermogravimetric analysis (TGA) analysis and dynamic mechanical analysis (DMA). The obtained polymer nanocomposite film was also examined in view of surface coating material with antibacterial effect against Gram-positive, Gram-negative, and Spore forming bacteria. It was demonstrated that nanocomposite samples exhibited coating materials with antibacterial effect against these bacteria. Additionally, the film properties of the nanocomposites were also determined and compared with those of the classical styrenated oil samples.

2. THEORETICAL PART

2.1 Triglyceride Oil

Triglyceride oils, which can be derived from both plant and animal sources, are found in abundance in all parts of the world, making them an ideal alternative chemical feedstock. These oils are predominantly made up of triglyceride molecules, which have the structure shown in Figure 2.1. Triglycerides are composed of three fatty acids joined at a glycerol juncture. Most common oils, such as corn, olive, soybean, and linseed oil, contain fatty acids that vary from 14 to 22 carbons in length with 0 to 3 cis-double bonds per fatty acid [26]. In Table 2.1., the fatty acid distributions of several common oils are shown [27]. The unsaturation in a fatty acid is typically found in a 1,4-pattern and thus, occurs at the 9,12, and 15 carbon positions relative to the carbonyl. Trans-configured bonds generally only result if the oil is subjected to a hydrogenation reaction. While double bonds are the dominant functionality of the fatty acid, other functional groups including fluoro, hydroxy, keto, or epoxy, have been found to naturally occur [26]. Two such examples are vernolic acid, which is a component of vemonia oil, and ricinoleic acid, which is a component of castor oil. Vernolic acid contains natural epoxy groups while ricinoleic acid contains hydroxyl groups [26].

Due to the many different fatty acids present, it is apparent that on a molecular level these oils are composed of many different types of triglycerides with numerous levels of unsaturation [28]. Figure 2.2 shows the double bond functionality distribution for three common oils, olive, soybean, and linseed oil. With newly developed genetic engineering techniques, it is possible to control this distribution as well as initiate the expression of new functionalities into plants. Generally, this is done by changing the amount of oleic acid in the oil. Oleic acid (18 carbons, 1 double bond) is considered to be healthy, due to the single unsaturation, but does not have the extreme instability of highly unsaturated fatty acids. With this control, it

would be possible to produce better materials by changing the oil functionality, or reduce the number of chemical modifications done in-vitro.

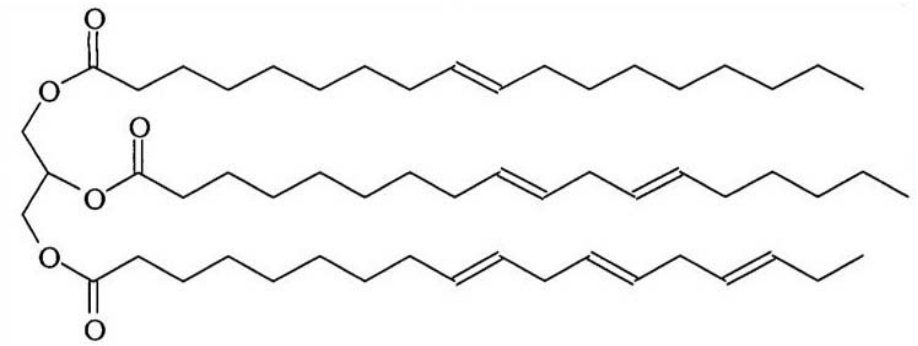

Figure 2.1 : Triglyceride molecule, the major component of natural oils.

The application of these oils in non-edible fields has primarily been confined to the paints, coatings and inks [29-31]. The small portion of applications that are in the polymers field use triglycerides as plasticizers or toughening agents. For example, epoxidized plant oils, such as epoxidized soybean oil (ESO), are a popular plasticizer/stabilizer for vinyl plastics, such as polyvinyl chloride, contributing almost 15% of the United States plasticizer market [32]. They provide many advantages over petroleum-based phthalate plasticizers, such as dioctyl phthalate, including a resistance to surface migration, leaching, evaporation, and light degradation. Although epoxidized soybean oil is more expensive than many petroleum based plasticizers, it is still a competitive alternative because of these properties.

Epoxidized triglycerides have also been examined as a toughening agent in epoxy polymers. Extensive work by Frischinger et al. studied the incorporation of epoxidized triglycerides, both epoxidized soybean oil and vernonia oil (oil with natural epoxy functionality) into diglycidyl ether of bisphenol A (DGEBA) [33,34]. Their results indicate that the reactivity of triglyceride epoxies is much lower than that of the DGEBA. Consequently, cure of a blend of DGEBA/ESO with an amine would result in liquid drops of epoxidized soybean oil dispersed within an epoxy network. Successful toughening of the epoxy resulted only when the epoxidized soybean oil was first oligomerized with a diamine and then blended with the epoxy at varying compositions. The resulting blends showed stress intensity factors, K_{IC}, almost twice that of the unmodified epoxy and fracture energies, G_{IC}, almost five

times that of the unmodified epoxy. The rheologicial and thermal behavior of these polymers was later characterized by Mustata and coworkers [35].

Table 2.1 : Fatty acid distribution in various plant oils

Fatty Acid	# C: #	Corn	Cotton	Linseed	Olive	Palm	Rapesee	Soybean
Myristic	14:0	0.1	0.7	0.0	0.0	1.0	0.1	0.1
Myristoleic	14:1	0.0	0.0	0.0	0.0	0.0	0.0	0.0
Palmitic	16:0	10.9	21.6	5.5	13.7	44.4	3.0	11.0
Palmitoleic	16:1	0.2	0.6	0.0	1.2	0.2	0.2	0.1
Margaric	17:0	0.1	0.1	0.0	0.0	0.1	0.0	0.0
Margaroleic	17:1	0.0	0.1	0.0	0.0	0.0	0.0	0.0
Stearic	18:0	2.0	2.6	3.5	2.5	4.1	1.0	4.0
Oleic	18:1	25.4	18.6	19.1	71.1	39.3	13.2	23.4
Linoleic	18:2	59.6	54.4	15.3	10.0	10.0	13.2	53.2
Linolenic	18:3	1.2	0.7	56.6	0.6	0.4	9.0	7.8
Arachidic	20:0	0.4	0.3	0.0	0.9	0.3	0.5	0.3
Gadoleic	20:1	0.0	0.0	0.0	0.0	0.0	9.0	0.0
Eicosadienoi	20:2	0.0	0.0	0.0	0.0	0.0	0.7	0.0
Behenic	22:0	0.1	0.2	0.0	0.0	0.1	0.5	0.1
Erucic	22:1	0.0	0.0	0.0	0.0	0.0	49.2	0.0
Lignoceric	24:0	0.0	0.0	0.0	0.0	0.0	1.2	0.0
Average	triglyc.	4.5	3.9	6.6	2.8	1.8	3.8	4.6

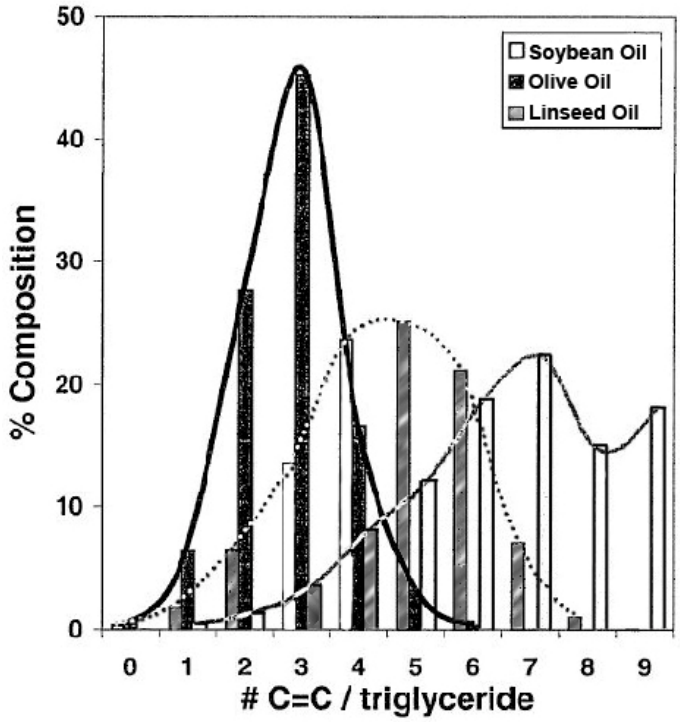

Figure 2.2 : Triglyceride double bond distribution for soybean, olive and linseed oils.

Rosch and Mulhaupt used various carboxylic acid anhydrides to cure epoxidized soybean oil, producing materials ranging from flexible rubbers to rigid polymers depending on the type of anhydride used [36]. The rigid polymers displayed glass transition temperatures (Tg) in the range of 43-73 °C. The highest Tg's were obtained when the epoxidized soybean oil was cured with maleic anhydride or phthallic anhydride. They utilized these polymers as toughening agents in polypropylene by curing the triglycerides in a polypropylene melt. Phase-separation would occur resulting in triglyceride domains in the 100-800 μm size range dispersed in the polypropylene. However, due to poor adhesion between these domains and the polypropylene phase, there was no toughening effect. In fact, the observed yield stress of the material was actually less than that of pure polypropylene.

Triglycerides have also been used to produce interpenetrating polymer networks in thermoset polymers. As reviewed by Barrett and coworkers, there are numerous types of triglycerides that can be used to produce interpenetrating networks [37]. Initially, castor oil, a hydroxy functional triglyceride, was used to produce interpenetrating polyurethane networks in polystyrene [38-40].

Acrylated epoxidized triglycerides have been used only in the coatings and ink industries. Due to their low-temperature curability and low volatile organics emission, these materials are favorable for such applications. Acrylated epoxidized triglycerides have been used for ultra-violet light curable coatings [31]. Other sources can be found in the literature for the application of acrylated epoxidized triglycerides for inks and coatings.

In all of the aforementioned work, the functional triglyceride was a minor component in the polymer matrix acting solely as a modifier to improve upon the main matrix's physical properties. Consequently, the triglyceride based materials were low molecular weight, lightly crosslinked materials, incapable of displaying the necessary rigidity and strength required for structural applications. Within the past few years, there has been much interest in producing materials where the triglyceride is a major component of a polymer matrix, and the polymer displays the necessary rigidity and glass transition temperature for engineering applications.

It is possible for the triglyceride to be polymerized in its natural form. Li and coworkers showed that the double bonds of the triglyceride can be used in their natural or conjugated form to form crosslinked polymers via cationic polymerization of the double bonds in the presence of a reactive diluents [41-44]. However, it is also possible to modify the triglyceride such that other techniques for polymerization, such as condensation, free-radical, or ring opening polymerization can be used.

2.1.1 Synthetic pathways for triglyceride based monomers

Over the past five years, the Affordable Composites from Renewable Sources (ACRES) program at the University of Delaware has developed a broad range of chemical routes to utilize natural triglyceride oils as a basis for polymers and composite materials [45]. The triglyceride contains active sites amenable to chemical reaction. These are the double bonds, the allylic carbons, the ester groups and the carbons alpha to the ester group. These active sites can be used to introduce polymerizable groups on the triglyceride using the same synthetic techniques that have been applied in the synthesis of petrochemical based polymers. The key step is to reach a high level of molecular weight and crosslink density, as well as incorporate chemical functionalities known to impart stiffness in a polymer network (e.g. aromatic or cyclic structures). Several synthetic pathways have been found to accomplish this as illustrated in Figure 2.3 [45].

Structures 5, 6, 7, 8 and 11 shown in Figure 2.3 use the double bonds of the triglyceride to functionalize the triglyceride with polymerizable chemical groups. From the natural triglyceride, it is possible to attach maleates or convert the unsaturation to epoxies or hydroxyl functionalities [46,47].

Epoxy functional triglycerides can be cured in the same manner as petroleum based epoxies (although, as mentioned earlier their reactivity is slightly less than conventional epoxy resins which have terminal epoxies). Curing agents such as polyfunctional amines, acid anhydrides, Lewis acids, or phenols can be used to cure these triglycerides producing materials with a wide range of properties. Hydroxyl functional triglycerides can also be cured by reactants such as polyisocyanates, anhydrides, and epoxies.

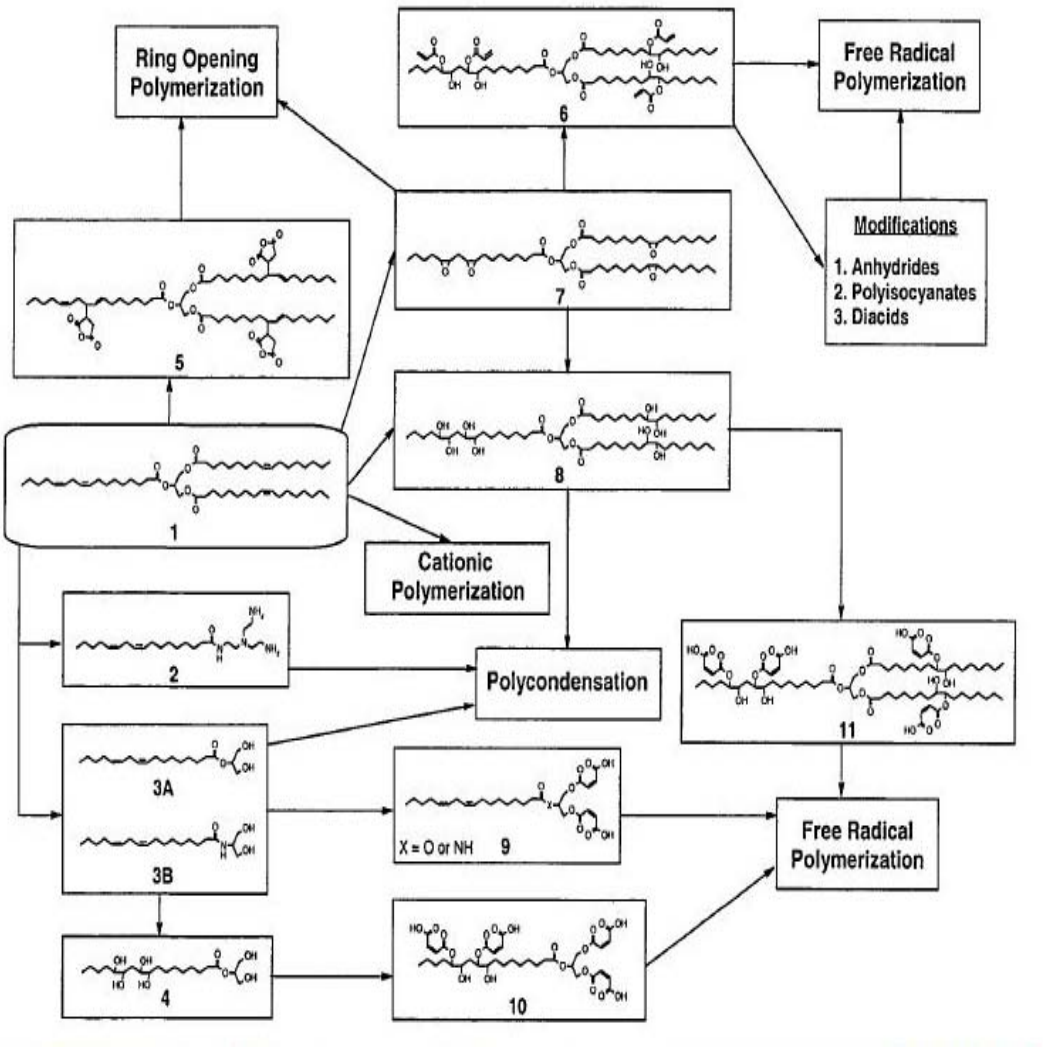

Figure 2.3 : Chemical pathways leading to polymers from triglyceride molecules.

It is also possible to attach vinyl functionalities to the epoxy and hydroxyl functional triglycerides. Reaction of the epoxy functional triglyceride with acrylic acid incorporates acrylates onto the triglyceride, while reaction of the hydroxylated triglyceride with maleic anhydride incorporates maleate half-esters and esters into the triglyceride. These monomers can then be blended with a reactive diluent, such as styrene, similar to most conventional vinyl ester resins and cured by free-radical polymerization.

The second method for synthesizing monomers from triglycerides is to convert the triglyceride to monoglycerides through a glycerolysis reaction or an amidation reaction [48-50]. Monoglycerides have found much use in the field of surface

coatings, commonly referred to as alkyd resins, due to their low cost and versatility. In those applications, the double bonds of the monoglyceride are reacted to form the coating. However, monoglycerides with either an amine functionality or hydroxyl functionality are also able to react through polycondensation reactions with comonomers, such as a diacids, epoxies, or anhydrides. Alternatively, maleate half esters can be attached to these monoglycerides allowing them to free-radically polymerize.

The third method is to functionalize the unsaturation sites as well as reduce the triglyceride into monoglycerides. This can be accomplished by glycerolysis of an unsaturated triglyceride, followed by hydroxylation, or by glycerolysis of a hydroxy functional triglyceride. The resulting monomer can then be used in polycondensation reactions by reaction with diacids, epoxies, or anhydrides. Alternatively, it can be reacted with maleic anhydride forming a monomer capable of polymerization by free-radical polymerization.

Due to the vast number of functionalities that can be added to the triglyceride, it is also possible to blend some of the above mentioned triglycerides with complementary functional triglycerides. For example, the hydroxyl functional monoglycerides or triglycerides can be used to react with epoxy functional triglycerides or anhydride functional triglycerides. Additionally it may be possible to form interpenetrating networks of flexible triglyceride networks with more rigid triglyceride based networks. For example an epoxidized triglyceride cured with a diamine in the presence of an acrylated triglyceride cured free-radically by reaction with a comonomer such as styrene. These are just a few examples of the many possibilities available to produce different materials with a wide variety of properties.

2.1.2 Internal unsaturation and auto-oxidative polymerization

Vegetable oils are classified into 3 categories, namely, drying oils (harden to a tough, solid film upon exposure to air), semi-drying oils (partially harden when exposed to air), and non-drying oils (remain tacky even upon prolonged exposure to air). The drying ability of vegetable oils is quantified and dependent upon their specific iodine values. Iodine value is defined as the mass (in grams) of iodine that is absorbed via

reaction with unsaturation by 100 g of vegetable oil. Drying oils such as tung, oiticica, linseed, and perilla have iodine values greater than 150 g/100 g of oil. Semi-drying oils such as soybean, sunflower, safflower, and tall oil have iodine values between 120-150 g/100 g of oil. Non-drying oils such as castor oil and coconut oil have iodine values of less than 120 g/100 g of oil [49].

Drying oils form tack-free films via oxidative crosslinking. Auto-oxidative polymerization proceeds through two stages: primary and secondary oxidation. These two stages encompass six main steps which include [51] :

- Induction period
- Initiation
- Hydroperoxide formation
- Hydroperoxide decomposition
- Crosslinking
- Formation of low molecular weight byproduct

Vegetable oils contain natural antioxidants such as a and (3-tocopherols, which inhibit oxidation through radical scavenging reactions. When the antioxidants are consumed, oxygen will abstract allylic hydrogen atoms creating resonance stabilized allylic radicals. Oxygen uptake and hydroperoxide (both cyclic and acyclic) [52] formation are accompanied by an increase in the degree of double-bond conjugation. The resultant allylic radicals quickly react with oxygen to form peroxy radicals. Secondary oxidation occurs next, characterized by loss of unsaturation and C-C and C-O-C bond formation via peroxide decomposition leading to radical recombination and double bond addition reactions [53]. Metal driers accelerate auto-oxidation by decreasing the activation energy for hydroperoxide decomposition via redox mechanisms [54]. Cobalt and manganese salts function almost exclusively as primary driers in curing the coating surface, whereas zirconium and calcium salts serve as secondary driers promoting even drying throughout the bulk film. Not all of oxidation reactions lead to crosslinks however. P-scission reactions between alkoxy radicals and fatty acids form low molecular weight products such as alcohols, ketones, carboxylic acids, and aldehydes. The putrid smell associated with the later stages of vegetable oil oxidation has been ascribed to aldehyde formation. Primary and secondary oxidation is illustrated in Figures 2.4 and 2.5, respectively.

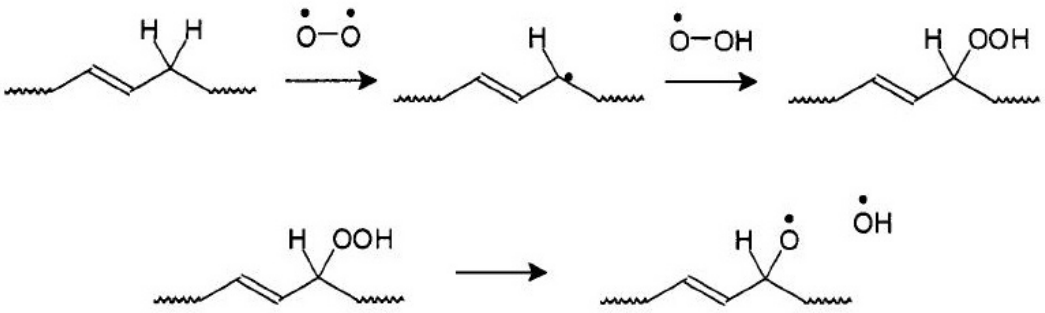

Figure 2.4 : Primary auto-oxidation reaction mechanism.

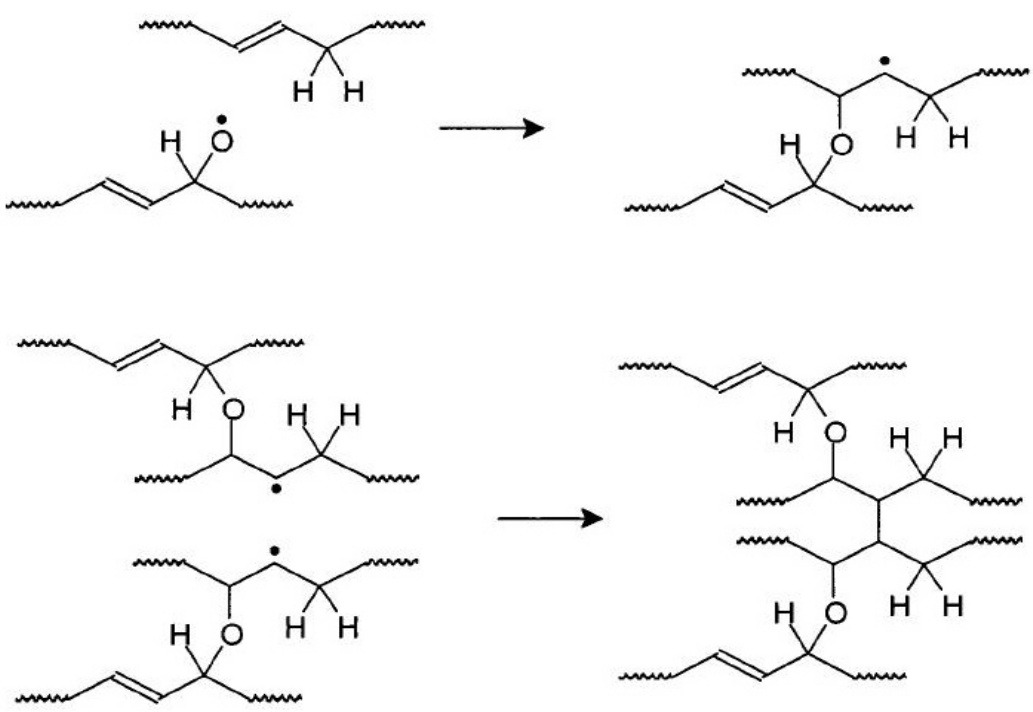

Figure 2.5 : Secondary auto-oxidation reaction mechanism.

2.1.3 Coatings applications for vegetable oils

Vegetable oils have a long history as binders for coatings, dating back to the 2nd century when the Greek physician Galen mixed oils with white lead, litharge, and umber. However, it was not until 1440 when the first varnishes were formulated with linseed oil that vegetable oils were used as protective coatings. Alkyds, or oil-modified polyesters, emerged in the late 1920's and are still widely used today but have been replaced in many applications by other synthetic resins. Nevertheless, alkyds continue to be the subject of significant research and new product development, as revealed by the alkyd patent histogram shown in Figure 2.6.

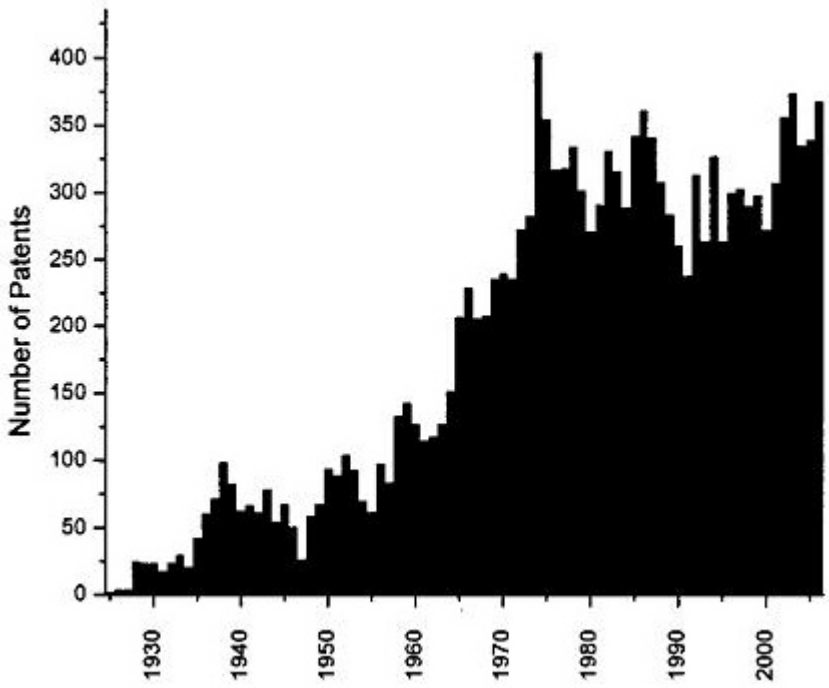

Figure 2.6 : Alkyd patent histogram.

Alkyds consist of vegetable oils/fatty acids, polyols, and polybasic acids, and are synthesized either through the fatty acid (FA) process or the monoglyceride (MG) process (Figure 2.7). The fatty acid process is more expensive because fatty acids have to be isolated from vegetable oils, and stainless steel or glass reactors must be used for esterification. However, this process offers great flexibility in altering the alkyd fatty acid composition to tailor performance properties. The monoglyceride process is less expensive, but the final alkyd always includes a mixture of fatty acids inherent to the vegetable oils used in the synthesis, and tuning the drying properties is therefore more difficult. Alkyds are versatile in performance, easy to modify, and are cost effective, but they have limited hydrolytic stability and tend to yellow with time. Although 100% solids alkyds are commercially available, most alkyds are thinned with solvents to reduce their viscosity and inherently contain volatile organic compounds (VOCs).

Waterborne coatings employ water as the continuous phase, and encompass emulsions (latexes), water-soluble resins, and water-dispersible systems, with emulsions being the most widely used of the three. These coatings offer the advantages of environmental friendliness, low toxicity, reduced fire hazards, and ease of cleanup and application. Latex research has grown in importance since the mid-1930's to meet the U.S. demand for synthetic

rubber during World War II, and rose dramatically in the 1960's when greater understanding of emulsion polymerization and reduction-to-practice fueled commercialization. Figure 2.8 shows the patent histogram for latexes, representing all latex applications, including coatings.

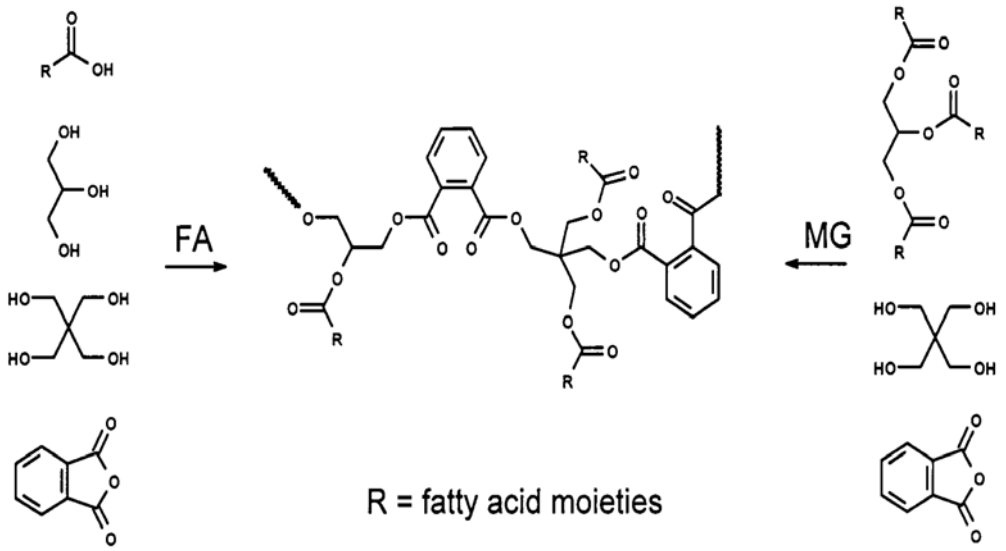

Figure 2.7 : Alkyd synthesis.

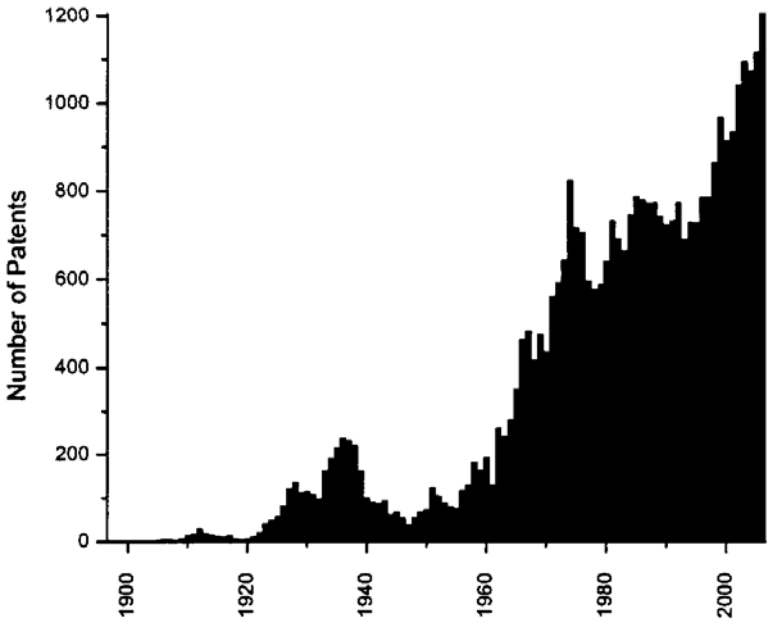

Figure 2.8 : Latex patent histogram.

In addition to alkyd and emulsion coatings, vegetable oils have also found application in UV curable materials. Epoxidized soybean oil has been used as the prepolymer component in cationic photopolymerization systems. Ultraviolet (UV) and electron beam (EB) curable materials fall under the class of radiation curable systems. UV coatings are more widely used than EB systems and will be the focus of this discussion. These materials had their beginning in coating flat wood products but now are extensively used in applications such as electronics, fiber optics, compact discs, and high-gloss magazine covers. The patent histogram for UV curable materials is shown in Figure 2.9.

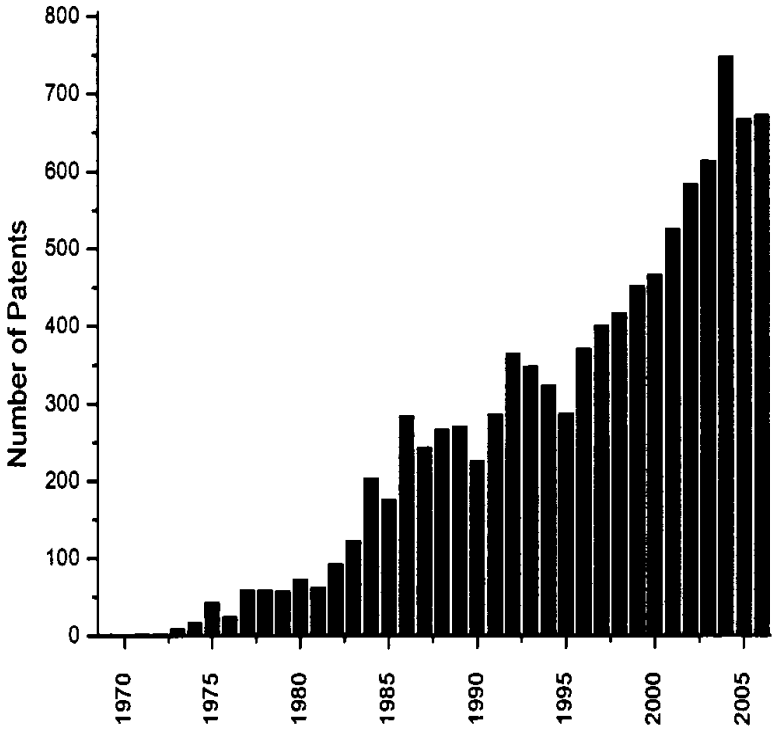

Figure 2.9 : UV curable patent histogram.

The sale and utilization of UV curable materials has grown steadily since the 1970's. Typical UV curable technology is 100% solids and capable of almost instantaneous curing. The rapid transformation from liquid to solid films under ambient conditions permit productivity advantages over alternative technologies such as increased line speed, reduced energy consumption, and lower space requirements [55]. Currently, UV curable coatings can be processed at rates up to 1000 ft/min.

Commercial UV curable coatings employ either free-radical or cationic chain-growth polymerizations, depending on monomer and photoinitiator choice. A less utilized but exciting technology are thiol-ene based materials, which polymerize via a step-growth mechanism that almost completely eliminates oxygen inhibition. Often the offensive odor resulting from the presence of small amounts of low molecular weight thiol impurities have hindered their commercial development. UV curable coatings consist of photoinitiators, reactive diluents, prepolymers (oligomers), pigments/additives, and a UV light source. Free-radical photoinitiators generate radicals through either a unimolecular (Type I) or bimolecular (Type II) process [56, 57]. Type I initiators, such as Darocur 1173, are alpha-cleavage benzoin alkyl ethers (Figure 2.10). Type II initiators are benzophenone systems and produce radicals by either sensitizing a co-initiator (Irgacure 500) or by abstracting hydrogen atoms from a donor amine (Figure 2.10).

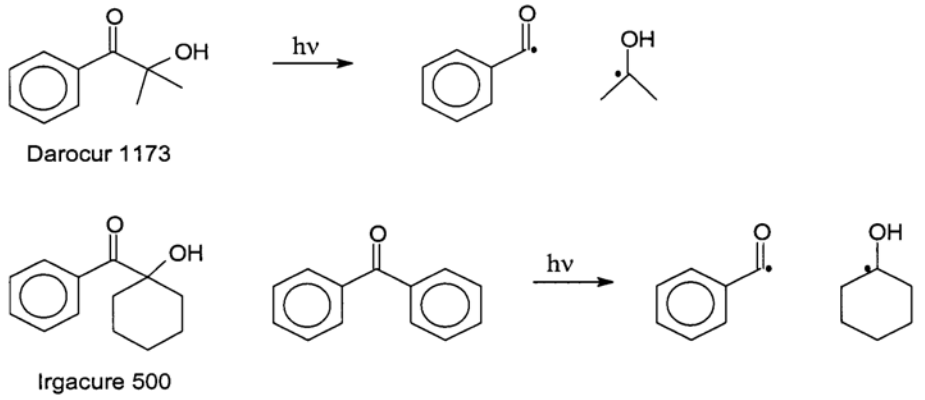

Figure 2.10 : Darocur 1173 and Irgacure 500 structures and decomposition products.

Common cationic photoinitiators include sulfonium (such as UVI® 6974) and iodonium salts that form superacids when irradiated with UV light (Figure 2.11).

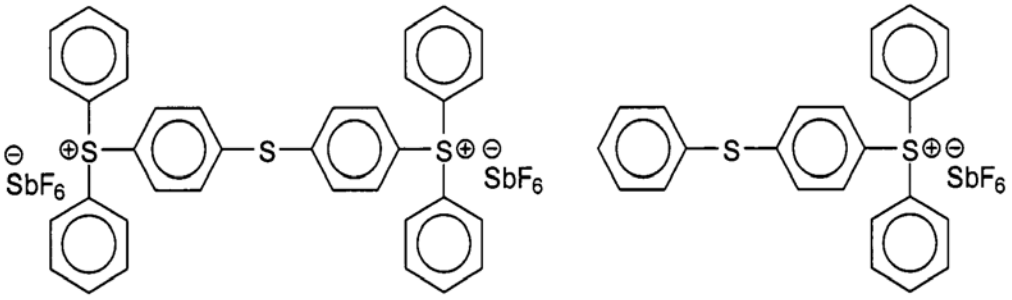

Figure 2.11 : UVI 6974 Photoinitiator structure.

Reactive diluents are low molecular weight mono- and/or multifunctional materials used to adjust the viscosity of UV curable coatings and copolymerize with the prepolymer upon UV irradiation. Common reactive diluents include (meth)acrylates, styrene, vinyl ethers, and cycloaliphatic epoxides (Table 2.2.). Crosslink density and cure rate increases with the degree of functionality. However, as functionality increases, the onset of vitrification (gelation) occurs at lower conversions and leads to incomplete functional group conversion. Therefore, a balance must be engineered between crosslink density, cure rate, and conversion.

Table 2.2 : Reactive diluents.

Name	Functionality	MW(g/mol)	Structure
Styrene	1	104	
Methyl acrylate	1	86	
1,6-Hexanediol diacrylate	2	226	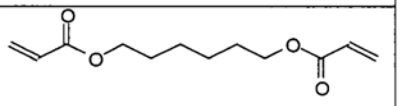
Trimethylolpropane triacrylate	3	282	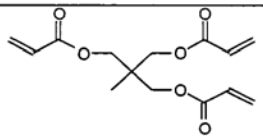
Pentaerytritol tetraacrylate	4	352	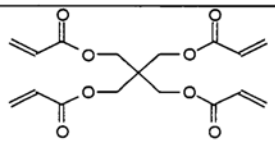
UVR-6105	2	252	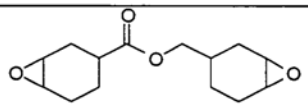

Prepolymers (Table 2.3) are the primary film formers in UV curable coatings and often dictate the coating's final properties. They range in molecular weight from several hundred to several thousand atomic mass units and are generally (meth)acrylate end-terminated epoxies, polyethers, polyesters, and polyurethanes for free-radical polymerizations and diglycidyl ether of bisphenol-A resins and derivatives for cationic polymerizations. Epoxidized seed oils such as epoxidized soybean and epoxidized linseed oils have also been used as prepolymers for cationic polymerizations [58].

Table 2.3 : UV curable polymers.

Name	General Structure
Acrylated urethane	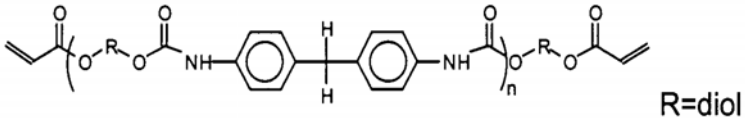 R=diol
Acrylated epoxide	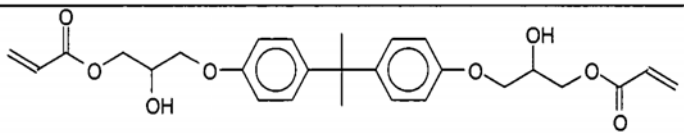
Acrylated polyester	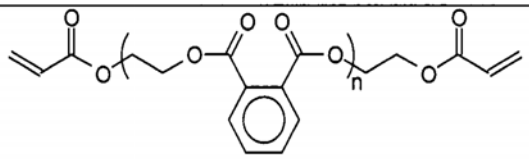
Acrylated polyether	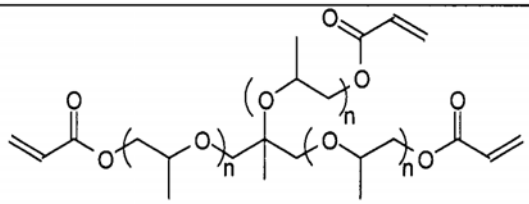
DGEBA	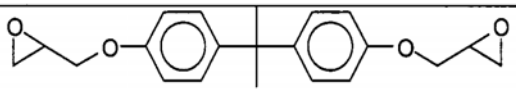
Epoxidized oil	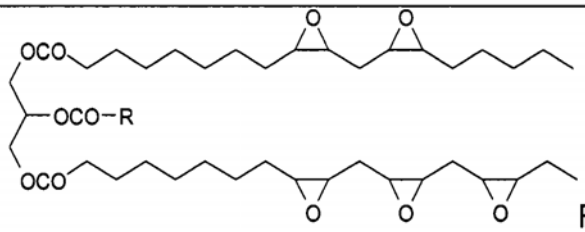 R=fatty acid

Pigments and additives are added in smaller quantities than oligomers and reactive diluents and present challenges in formulation of UV curable coatings because they are also capable of absorbing UV light. This is especially true if formulating with a UV stabilizer or with a pigment such as titanium dioxide, which absorbs all wavelengths of UV light below 400 nm. Competitive absorption of photons leads to a reduction in the number of radicals/cations available to initiate polymerization, and limits the extent of cure. Several solutions have been suggested for this problem, the most practical being a judicious choice of photoinitiator and light source. The photoinitiator's absorption profile must sufficiently overlap with the light source's emission bands and lie outside the absorption profile of the pigment and additive. For

TiO_2 pigmented coatings, a photoinitiator which absorbs at longer wavelengths (in the visible spectrum) is generally used.

Light sources employed in UV curable coatings include mercury vapor lamps (low, medium, and high pressure), pulsed xenon lamps, doped mercury lamps, electrodeless lamps, lasers, and light emitting diodes. The sources vary in emission wavelengths, emission intensity, power consumption, and bulb cost. Medium pressure mercury lamps are the most widely used light source, as they are relatively inexpensive, less hazardous than other bulb types, and have a wide emission spectrum. These lamps emit both high energy light (254 nm) to cure the coating surface and low energy light (366 nm) that deeply penetrate and cures the bulk of the coating.

2.2 Polymer Chemistry

A brief introduction into various aspects of polymer chemistry, in particular the synthesis of polymers via free radical polymerization, will be presented in this section.

In the world of materials, civilization has progressed from utilizing simple wood and stone to the development of metallurgy. Beginning in the early 1900's scientists began synthesizing plastics which lead to the birth of a new age. Since the 1950s, plastics have grown into a major industry that affects all of our lives -- from providing improved packaging and new textiles, to permitting the production of wondrous new products and cutting edge technologies. Plastics even allow doctors to replace worn-out body parts, enabling people to live more productive and longer lives. In fact, since 1976, plastic has been the most used material in the world. Plastics, elastomers, coatings and adhesives are some of the few classes belonging to the group of materials known polymers.

A synthetic polymer by definition is a large molecule made up of repeating units with a molecular weight of at least 100 times greater than that of the repeating unit. Homopolymer is made up of one repeating unit; whereas, a copolymer is made of two or more repeating units. Polymers may be synthesized either by an addition polymerization or a condensation polymerization reaction. In this section chain-

reaction addition polymerization will be considered using free radical initiation and photoinitiation of vinyl monomers.

2.2.1. Free radical polymerization

A few monomers can polymerize on heating without the aide of an initiator; however, most monomers require an initiator to jump start the polymerization process. Free radical initiators can be, but are not limited to, peroxides, hydroperoxides, azo compounds such as azobis(isobutyronitrile) (AIBN), and benzoins such as 2-hydroxy-2-methyl-1-phenyl-1-propanone (Benacure 1173, Mayzo). Initiators can decompose to produce free radicals either thermally or photolytically. Figures 2.12, 2.13 and 2.14 show the decomposition of benzoyl peroxide (BPO), α,α,-azobis(isobutyronitrile) , and 2-hydroxy-2-methyl-1-phenyl-1-propanone (Benacure 1173, Mayzo), respectfully [59].

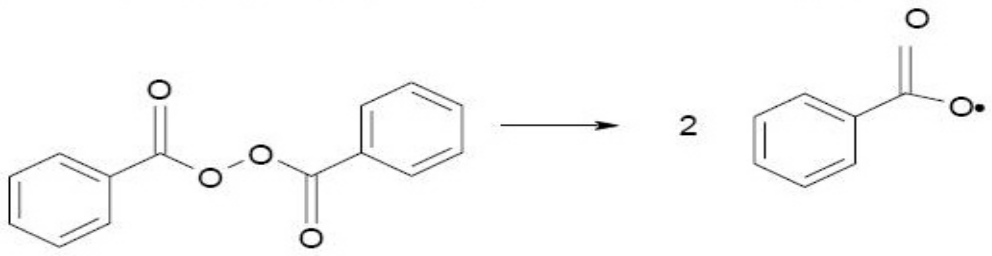

Figure 2.12 : Thermal decomposition of benzoyl peroxide to the benzoyloxy free radical.

Figure 2.13 : Thermal decomposition of α,α,-azobis(isobutyronitrile) to the dimethylcyano free radical.

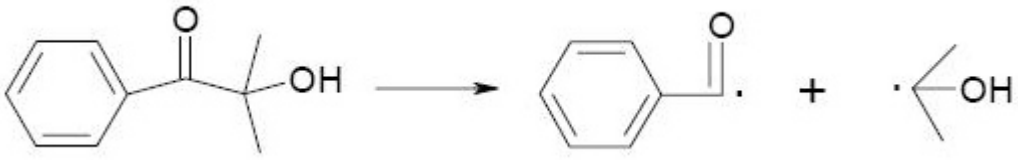

Figure 2.14 : UV decomposition of 2-hydroxy-2-methyl-1-phenyl-1-propanone (Benacure 1173, Mayzo).

Once the initiator has decomposed to produce the free radical, the free radical reacts with a vinyl monomer or a strained-ring cyclic monomer to begin the initiation step of polymerization. Figure 2.15 shows the initiation of styrene monomer using the benzoyloxy free radical.

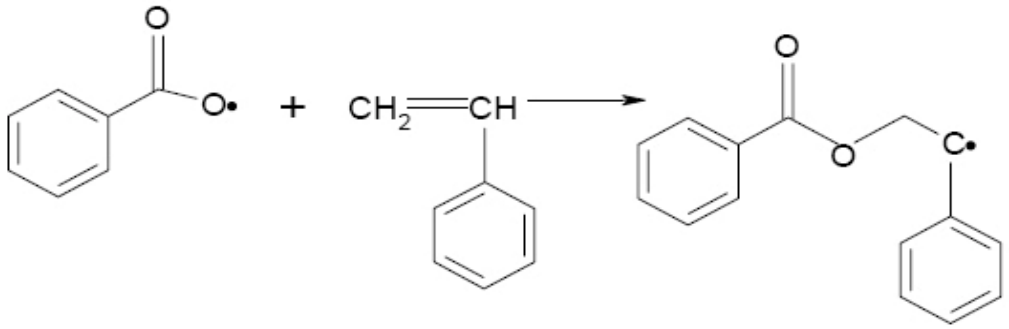

Figure 2.15 : Free radical initiation of styrene monomer.

This step is then followed by a propagation step where the radical activated monomer reacts with a monomer unit to begin building the polymer chain. This step is shown in Figure 2.16.

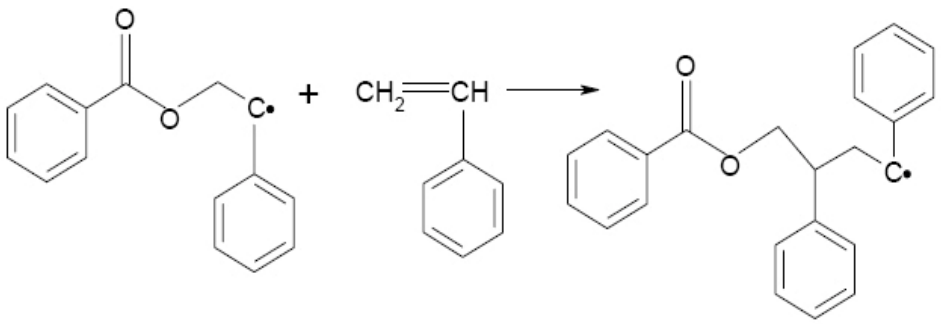

Figure 2.16 : Propagation of a polystyrene chain.

Termination of a polymer chain via coupling and disproportionation is shown in Figure 2.17.

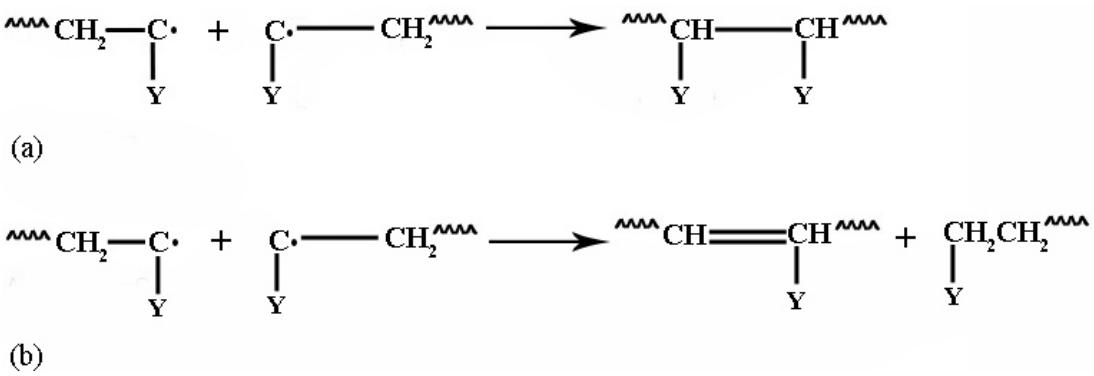

Figure 2.17 : Termination of a polymer chain via (a) coupling and (b) disproportionation.

2.2.2 Photopolymerizations based on free radical mechanism

Photoinitiated free-radical polymerization offers compelling advantages over traditional thermal polymerization, including low energy consumption, room temperature curing, high speed under mild conditions, spatial and temporal control and solvent free polymerization, among others. Instead of thermal-induced generation of initiating species, these photo-induced processes invariably include a light-absorbing compound that is capable of creating active centers directly or photosensitizing the generation of such active centers upon irradiation. The beneficial features of photopolymerization were first demonstrated in a number of thin film applications such as coatings, paint, and varnishes. Compared with thermal drying in which the evaporation of the solvent often results in an uneven surface and a loss of sample thickness, the solvent-free photopolymerization can easily achieve a significantly enhanced surface smoothness and much lower degree of shrinkage. In recent years, significant advantages have been accomplished in the development of photopolymerization as a result of the innovative designing of highly efficient photoinitiation systems and the implementation of newly emerged radiation technology, such as lasers. These new advancements make it possible to apply the photo-induced polymerization to a much broader set of technologies that require fast-curing and low toxicity in room temperature (e.g., biomaterials, imaging, optics, stereolithography, etc.). Photopolymerization differentiates itself from thermal polymerization by using specific forms of radiation (UV/Visible) as an energy source

to initiate the decomposition of initiators or excite the photosensitizers. As a result, improving the efficiency of photoinitiators to convert the absorbed light energy to chemical energy (which leads to bond dissociation, electron/proton transfer, etc.) has become an important consideration in the design of photopolymerizable systems. In addition, specific requirements (such as low shrinkage, flexibility, fast curing rate, and constraints on particular physical properties) imposed by a variety of industrial applications lead to the development of different initiation systems with unique features and advantages. For example, free radical chain reactions are generally attributed with high reaction speed, wide selection of commercially available monomers, and relatively low cost and toxicity, while the cationic chain reactions are well known for their low shrinkage and inertness to oxygen inhibition. In recent years, thiol-ene type polymerizations have seen significant growth both in scientific research and industry due to their rapid reaction, immunity to oxygen inhibition and versatile properties of polymerized products. The mechanism of free radical photopolymerization is well established and can be outlined as:

Photoinitiation: It is based on absorption of light by a photosensitive compound or transfer of electronic excitation energy from a light absorbing sensitizer to the photosensitive compound.Homolytic bond rupture results in the formation of a radical that reacts with one monomer unit. This step is the only difference between photopolymerization and thermal radical polymerization.

Propagation: It is repetitive addition of monomer units to the chain radical producing the polymer backbone.

Chain transfer: It is termination of growing chains via hydrogen abstraction from various species like solvent and accompanying production of a new radical capable of initiating another chain reaction.

Termination: Polymeric radicals are used up by coupling or disproportionation reactions. Four steps of photopolymerization are summarized in Figure 2.18.

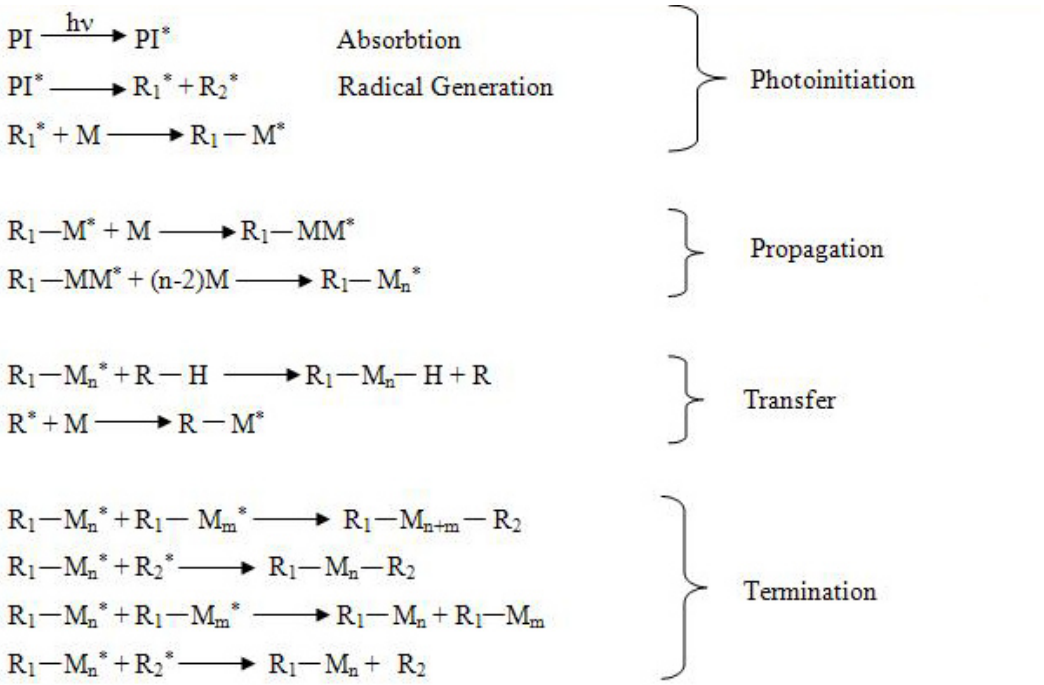

Figure 2.18 : Four steps of photopolymerization.

Most of the unimolecular cleavage initiators contain a benzoyl group and an alkylaryl or heterosubstitute. There are two typical electronic transitions for these aromatic carbonyl molecules: and $\pi \to \pi^*$,which will lead to the formation of two excited singlet states: $S_1(n\pi^*)$ and S_2 $(\pi\pi^*)$ Although the $\pi \to \pi^*$ transition is symmetry forbidden, the occurrence of such processes is facilitated in carbonyl groups due to the presence of the heteroatom - oxygen. The intersystem crossings from the excited singlet states to corresponding triplet states are highly efficient due to the small energy gap. When compared with excited singlet states, the triplet states have a relatively long lifetime, as a result, most of the cleavage reactions start from the excited triplet states of photoinitiators. The benzoyl radical formed from the decomposition of the photoinitiator is the major initiating species; the substituent radicals can either initiate polymerization directly or undergo further decompositions to create initiating radicals. The unimolecular cleavage normally proceeds at high speed and is thus not likely to be affected by triplet state quenching of oxygen [60].

In contrast to the unimolecular cleavage initiation, hydrogen abstraction and electron transfer reactions require the presence of both photo sensitizer (typically a diaryl ketone or an organic dye as light absorbing agent) and coinitiators (hydrogen donor,

electron donor/acceptor). The $(n\pi^*)$ triplet state of the photosensitizer (diaryl ketone) is considered to play a more active role than the $(\pi\pi^*)$ triplet state in hydrogen-abstraction processes. The energy of the reactive triplet state is higher than the C-H bond energy of the hydrogen donor, this will lead to hydrogen transfer from the donor to the sensitizer, and the resulting donor radical is believed to be the reactive species which initiates polymerization. In the case of electron transfer reactions, the photosensitizer can participate in the process either as an electron donor or an electron acceptor. The exact role played by the sensitizer depends on the redox potential of the sensitizer and the coinitiator, as well as the energy of the absorbed photons. The electron transfer process is usually followed by a fragmentation to produce the initiating species. It is valuable to note that the process of energy transfer from the photosensitizer to the coinitiator is typically longer than the unimolecular cleavage process, therefore, the bimolecular system is more susceptible to various quenching processes as a result of prolonged lifetime of reactive excited states of the sensitizers [60].

Other free radical photoinitiation mechanisms include intramolecular reactions and multi-component initiation. The later generally consists of a combination of unimolecular and bimolecular reactions. Photosensitized cleavage of peroxide species to create active centers has also been reported.

2.3 Metal Polymer Nanocomposite

Formation of metal nanoparticles in a polymer matrix became a popular tool for design of new metal/polymer nanocomposites, the properties of which can be greatly altered compared to those of pure polymers [61]. Incorporation of nanoparticles into a polymeric system may impart magnetic, semiconductor, catalytic, or sensing properties, depending on the kind of nanoparticles, formed inside a polymer, and nanoparticle characteristics. To obtain metal/polymer nanocomposites with well-defined and well-reproducible properties, one should carry out a subtle control over nanoparticle growth, particle size distribution, and particle-interface interactions. These are key issues to the desired properties and targeted applications of polymeric materials. Narrow particle size distribution is especially crucial, since optical, magnetic, sensing, and even catalytic properties strongly depend on the precise

control over particle size. One of the prominent ways to control nanoparticle size and morphology is to employ functional polymeric nanostructures with well-defined interfaces [62-64]. These interfaces can be generated via hydrophobic–hydrophilic microphase separation; or, due to nanopores or nanocavities, they can be formed within a polymer during synthesis. The presence of functional groups able to interact with metal compounds allows incorporation of metal species into the functional nanophase, while subsequent reduction or thermal (or other) treatment results in nanoparticle formation within this restricted area. The characteristics of the functional nanophase, metal compound loading, type of reducing agent, and other parameters are responsible for metal nanoparticle and metal/polymer nanocomposite characteristics. The control of nanoparticle morphology becomes a very important aspect, since morphology profoundly influences the material performance. As a long-term goal the development of synthesis schemes able to control particle size, shapes, and composition independently from one another is very important, in order to allow tuning of nanocomposite properties.

Metal/polymer nanocomposites can be obtained by two different approaches, namely, *in situ* and *ex situ* techniques. In the *in situ* methods, metal particles are generated inside a polymer matrix by decomposition (e.g., thermolysis, photolysis, radiolysis, etc.) or chemical reduction of a metallic precursor dissolved into the polymer. In the *ex situ* approach, nanoparticles are first produced by soft-chemistry routes and then dispersed into polymeric matrices. Usually, the preparative scheme allows us to obtain metal nanoparticles whose surface has been passivated by a monolayer of *n*-alkanethiol molecules (i.e., C_nH_{2n+1}-SH). Surface passivation has a fundamental role since it avoids aggregation and surface oxidation/contamination phenomena. In addition, passivated metal particles are hydrophobic and therefore can be easily mixed with polymers. The *ex-situ* techniques for the synthesis of metal/polymer nanocompos-ites are frequently preferred to the *in situ* methods because of the high optical quality that can be achieved in the final product.

2.3.1 Synthesis methods for spherical metal nanoparticles

Nanotechnology is slowly emerging from its infant stages. Applications from this area of science are only just beginning to form and only in a rudimentary fashion. In order for this discipline of science to grow new nanoparticle samples need to be

available in large supply for study and integration into other materials. To make this into reality synthetic routes must be found to make nanoparticles from all types of materials. Control of the size of each type of particle will lead to the possibility for integration in new devices, and allow resourceful probing of their capabilities so they can become agents of technological advancement.

Spherical noble metal nanoparticles are an ideal material for a study of this scope. A sphere is identical in all aspects in space, when the size of these particles is changed only one dimension changes, and therefore a direct correlation between size and behavior can be determined. Geometrical triangles, rods, wires, and irregular particles contain more than one variable to account for and insinuations must be made. Moreover, noble metal nanoparticles are suitably stable for analysis and carry the potential to be involved in several exciting applications.

Many approaches to the synthesis of metal nanoparticles have been taken each with its own advantages and disadvantages. This ranges from the first documented formation of nanoparticles by reducing gold salts in solution to elaborate chemical vapor deposition apparatus that stabilize particles in inert gases. Unique and wonderful new nanoparticles often also call for extreme synthetic preparation methods. Scientists have gone to enormous lengths using many powerful techniques available including lasers, microwaves, and sonication to induce metal nanoparticle formation and produce high quality products. Other nanoparticle formation strategies developed have included photo-induced reduction of metal ions, bio-reduction, and use of versatile highly branched dendrimer macromolecules as nano-reactors.

2.3.1.1 Turkevich, brust, and the wet chemical reduction of nanoparticles

In 1951Turkevich and Stevenson made a fascinating study of the preparations of gold nanoparticles known at the time [65]. Reproducing the experiments themselves, the researchers compared the products on an early TEM. The pair also developed the optimal conditions for their own preparative scheme involving the citrate reduction of gold ions which proved not only the simplest method of the techniques investigated but yielded the best quality of particles as well. The citrate method is a very cheap and easy method of creating metal nanoparticles, and variations of this procedure are still in use today. The system has no waste products as the citrate molecules act as a

reductant and complexing agent in solution, eliminating the need for purification of the particles. Particles formed from this method are typically a little larger at 15-20 nm in diameter and have only a fair size distribution [65]. The method has been applied successfully to many methods such as silver, however since it is an aqueous system it is not amenable for use with some of the more reactive metals. Other variations on this method were later introduced in an attempt to manipulate the size of the particles.

Interest in metal colloids wanted for many years until the 1990's when the applications for nanoparticles began to drive an explosion of scientific interest that is currently thriving. Many other synthetic approaches similar to the Turkevich method were found that relied on reduction of metal salts in solution. The benefits of other reducing agents such as sodium borohydride [66,67] hydrazine [68], hydroxylamine hydrochloride [69], glucose [70], hydrogen gas, ethylene glycol [71], and long chain amines [72,73] were studied extensively. The power of the reducing agent had a direct dependence on the products, that were unique in size, shape, quantity, or quality of the colloid produced. Some methods favor products that can be dispersed in water, vs. organic solvents, while others could provide a reliable synthesis in which purification of the particles is not required.

The most famous of these techniques is the Brust method which utilizes a two-phase system and produces particles of 1-4 nm in diameter [74]. The Brust synthesis relies on a phase transfer agent tetraoctylammonium bromide (TOAB) to bring the unreduced gold salt $AuCl_4^-$ from the aqueous to the organic phase. The salt was then reduced by addition of sodium borohydride quickly forming nanoparticles in solution. These particles are protected from one another rapidly due to the immediate presence of dodecane thiol in the organic phase that stabilizes the particles from aggregation much like citrate ions in the Turkevich method. Dodecanethiol, however displays a much stronger binding to the metal center as the sulfur atom is a softer base and has a better interaction with the soft noble metal atoms than the acid moiety. This ligand is the standard molecule used in any new synthesis of metal nanoparticles today. The Brust synthesis provided the means to metal nanocrystals that were stable enough to isolate by precipitation from solution and study extensively, helping to drive the interest in this field of science.

More sophisticated syntheses were developed to control the immediate environment of the metal atoms as they are first reduced. One very successful and interesting wet chemical synthetic preparation is the creation of a microemulsion system, or inverse micelle liquid crystal within the solution to perform the reduction. By instituting a delicate balance between a surfactant and two solvents of drastically different polarities surfactant molecules order themselves much like a cell membrane into spherical pockets separating the aqueous and organic phases. The area inside each micelle is limited which encourages small particles. The separation between micelles prevents aggregation between particles when the reducing agent is introduced to the solution. This process has been shown to form particles with a very narrow size distribution demonstrated by Stoeva, and can be applied to many different metals [74]. Variations of this technique were applied with other solvents including an aqueous/ supercritical carbon dioxide (CO_2) system in which the micelles contained water but the solvent was CO_2. This also proved to be a successful synthetic method [75]. Unfortunately, the wet chemical reduction methods require purification of the nanoparticle product as the solution contains many excess ions that interfere with some of the particles properties.

2.3.1.2 Physical vapor deposition

The previous discussion has shown that the synthesis of metal nanoparticles via wet chemical methods is very reliable, quick, and at times can produce very monodisperse products with a fair degree of control over experimental conditions. However the amount of nanoparticles that can typically be made through this method is rather small, while requiring vast amounts of solvents. Also the presence of excess ions in solution may be problematic and can take away from the applicability of the product in many devices. Vapor deposition methods can bypass some of these problems. This synthesis typically involves the evaporation of a source material into a high vacuum and collecting the product after it has reacted with a stabilizing agent [76]. The experimental equipment required for this type of synthesis can often be elaborate, requiring very low pressures and high voltages. High purity products can be obtained through this process however, and the amount of nanomaterials produced can be increased greatly over solution chemistry approaches [76].

Physical vapor deposition (PVD) is typically used to produce thin films and coatings for the creation of many electrical components, antireflective coatings on optical equipment, or hard coatings on mechanical tools. Nanoparticulate metal powders can be created in this way as well. In fact almost any material can be atomized in such a reactor from many different forms (powder, rod, wire, ect.). Although there are several ways to evaporate the source material, thermally heating the sample from a tungsten crucible is the most common. The evaporated metal atoms or clusters can be cooled by a carrier gas such as helium to reduce reactivity, and then deposited on a cold finger. When the reaction is completed the powder can be scraped from the cold finger and can be composed of crystallites as small as 5-15 nm in diameter [76]. Where coatings are desired a free path to the substrate is optimal. PVD has the drawback in that if composite materials are desired the evaporation is not likely to be uniform due to different boiling points. Using lasers to evaporate the metal can overcome this deficiency, however it adds complexity to the reactors. Many composite materials can be produced if the reactor is slightly modified and gases such as oxygen, nitrogen, or hydrogen are allowed to react with the metal vapor to produce oxides, nitrides, and hydrides respectively through a process called chemical vapor deposition (CVD). An interesting variation of this method is the solvated metal atom dispersion (SMAD) method developed by Klabunde *et al* [77,78]. This procedure involves co-evaporating a metal source along with a stabilizing solvent that co-precipitate on a cold finger. If the solvent is in great enough excess to the material then the reactive atoms are stabilized and can be recovered by a controlled warming process where the atoms aggregate only slightly. The product can be polydisperse but is able to be refined by a process they developed termed digestive ripening [79]. Vapor deposition methods are difficult to set up, however the products obtained from them are often of very high quality, and can provide in situ information on the formation of the nanoparticles if spectroscopic attachments are incorporated into the reactor.

2.3.1.3 Synthesis of metal nanoparticles through sonication

Recently scientists have discovered that ultrasonication can be used to create extreme reaction conditions in liquid environments. The irradiation of liquids with sound waves produces acoustic cavitation where in localized, small areas of the solution enormous temperatures and pressures can be reached that can drive chemical

reactions in unique ways [80]. This technique has been applied to the synthesis of metal nanoparticles as well as the creation of nanoparticle oxides, sulfides, and unique polymer surfaces. Li and coworkers studied the effects of low-power ultrasonication to nanoparticle synthesis. During a typical sodium di-2-ethylhexylsulfosuccinate (AOT)/isooctane inverse micelle reduction of silver nanoparticles by $NaBH_4$, it was found that in the absence of sound waves the micelles created spherical reaction chambers. Reduction of silver ions in these micelles produced spherical silver nanoparticles. When the reaction vessel was sonicated during synthesis the shape of the micelle itself became ellipsoidal and caused aggregation of the particles inside the micelles. The morphology of the particles was shown to be dependent of the sonication time as nanorods and nanowires were formed with increasing sonication time respectively. The structure of the inverse micelles was followed through small-angle X-ray scattering studies [80].

The laboratories of Nagata expanded sono-chemical techniques to prepare bimetallic nanoparticles namely Au/Pd catalytic particles [81]. Their proposed reaction scheme involves the reduction of gold and palladium salts by radicals formed from the effects of sonication on the solution. In between the collapsing cavitation bubbles they suggest that hydrogen radicals form, which react with sodium dodecyl sulfate, the radicals of which reduce the metal. Core-Shell structures were found to form due to the lower reduction potential of gold vs. palladium.

2.3.1.4 Synthesis of metal nanoparticles through microwave ırradiation

The use of microwaves has been a recent advancement in chemical synthesis beginning in 1986 [82]. Similar to the use of sonication, microwave synthesis induces unique and extreme reaction conditions on the sample. Microwave irradiation causes rapid volumetric heating and has been found to drastically increase reaction rates. Kamarneni *et al* has adapted an efficient synthesis of silver nanoparticles using a two-phase liquid synthesis driven by microwave heating [82]. Their synthesis involves a toluene/ethylene glycol system with dodecanethiol added to the toluene layer. The synthesis is conducted in a Teflon container where the microwave irradiation sustains the reaction at 170 ºC for 3 h.

The nanoparticles obtained through this method were very monodisperse at roughly 10 nm in size, and displayed a high propensity to self-assemble. The synthesis through this method was simple, and allowed a relatively large amount of silver to be processed at once at 0.15 g silver nitrate. Many products could be achieved with this method, which is applicable to production of silver sulfide nanocrystals by adding thiourea to the reaction system. Nanocubes were even obtained by reducing the amount of dodecanethiol in solution with respect to the silver ion [82].

Gedanken applied microwave synthesis to the creation of bimetallic core-shell Au/Pd particles using the polyol synthesis [83]. The formation of gold is again attributed to the more favorable reduction of gold thermodynamically. The experimental setup of microwave reactions is simple, merely consisting of a microwave fixed with a water cooled condenser to prevent solvent loss during reaction [83].

2.3.1.5 Photo reduction

In an attempt to find a controllable procedure for a reproducible synthesis of metal nanoparticles some research groups have attempted the photochemical reduction of metal salts. Mallick et al. found that by irradiation of gold chloride in a solution of Triton-X they could reproducibly prepare a solution of seed nanoparticles [84] This precursor could then be used tocreate uniform colloids of larger particles by adjusting the amount of additional metal salt to nanoparticle seeds in solution. By this method the group was able to form particles of 35-40 nm, 55-65 nm, and 65-85 nm in diameter with the addition of greater amounts of free metal salt.

The mechanism of reduction is proposed to be an initial homolytic splitting of H_2O into hydrogen and hydroxide radicals by UV light. The radicals could either create a radical of Triton-X or reduce the metal in solution independently. The formation of a solution of seed crystals was found to be vital to production of quality colloids since the reduction potential of metal ions to metal atoms in the ground state is so much higher than the potential to reduce metal ions onto metal clusters. From this seed solution more metal atoms could be slowly deposited upon the surface of the crystallites with milder reducing agents, thus allowing for more controlled growth. The authors claim that synthetic methods that involve creation of seed crystals and growth simultaneously, are much more apt to result in polydisperse solutions, as new

seeds are constantly being created in solution and rapid agglomeration occurs from the use of harsh reducing chemicals. The authors have been able to apply this method to the synthesis of copper and silver metal particles as well as gold [84].

Work completed in El-Sayed's laboratory has also led to a synthetic procedure to create metal nanoparticles photochemically [85]. Their method involves the use of ethylene glycol as a reducing agent and poly(vinylpyrrolidone) (PVP) as a capping agent. By irradiation of 250-400 nm wavelength light the reaction can be driven at room temperature. From earlier observations and through studying the reaction kinetics (by UV-Vis absorption) with respect to the ethylene glycol mole fraction to gold salt they proposed the following mechanism for the photoreduction of gold salt (reactions 2.1a-e).

$Au^{(3+)}Cl_4^- \; h\nu \rightarrow [Au^{(3+)}Cl_4^-]^*$	Excitation	**(2.1a)**
$[Au^{(3+)}Cl_4^-]^*$ glycol $\rightarrow Au^{(2+)}Cl_3^- + Cl$	Reduction	**(2.1b)**
$2Au^{(2+)}Cl_3^- \rightarrow Au^{(1+)}Cl_2^- + Au^{(3+)}Cl_4^-$	Fast disproportionation	**(2.1c)**
$4Au^{(1+)}Cl_2^- \rightarrow 2Au^{(2+)}Cl_3^- + 2Au^0 + 2Cl^-$	Slow disproportionation	**(2.1d)**
Au^{+m} glycol $\rightarrow Au^0$ (+m :+3, +2, +1)	Glycol reduction	**(2.1e)**

The use of UV light has drastically cut down on the energy demands for the preparation of nanoparticles by this procedure, and forms a quality solution of nanoparticles. Under a different set of experimental conditions, irradiation of pre-formed spherical nanoparticles by low energy light sources was found to cause the growth of the particles into flat triangular nanoplates [86]. This reaction was observed to be caused by 350-700 nm wavelength laser light. Attempts at carrying out the reaction in the dark or with less energetic light resulted in no reaction. The formation of spheres into prisms is an interesting result that is most likely caused by the use of the surfactant Bis(p-sulfonatophenyl) phenylphosphine dihydrate dipotassium salt (BSPP) and may be aided by the presence of citrate ions in solution. While the reaction is driven or initiated by the light energy, the shape is more likely a result of the combination of surfactant molecules in solution. The synthesis of nanoparticles of various shapes and sizes has given researchers access to materials with further enhanced properties with more complex and less predictable results.

2.3.2 Characterization of metal nanoparticles

Nanoparticles were not first created in the last century, in fact many forms of materials have been of nanosize. However the technology to view and explore these materials was mainly lacking at the time leaving nanoparticles in a world of obscurity too small to have been noticed by science. The advent of imaging smaller materials has been possibly the greatest asset that has allowed contemporary scientists to fully engage the discipline of nanotechnology. This has provided a means to probe the size and morphology of these materials and to relate their size to their properties. There are three types of electron microscopes that are frequently reported in the literature to characterize nanoparticles, transmission electron microscopy (TEM), scanning electron microscopy (SEM), and atomic force microscopy (AFM).

2.3.2.1 Transmission electron microscope

TEM is one of the primary tools of the materials chemist and is almost essential to accurately describe the size, and shape of metal nanoparticles. Images from the TEM allow scientists to obtain the equivalent of X-ray negatives of a sample; higher density material shows up dark with a high contrast supported on a low density thin carbon film. An incident beam of electrons is created by running a potential across a filament (often tungsten) that can vary from 50-300 keV. The greater the voltage of the filament used the smaller the wavelength of the ejected electrons, and therefore a better resolution of the sample can be obtained.

Samples are typically placed on a thin metal grid covered by a plastic or carbon film that supports the sample to be viewed. This grid is then placed in the electron beam between the filament and a phosphorous plate that lights up as electrons hit the surface. Electrons localized on atoms in the sample will block the passage of the electron beam and appear as dark areas on an otherwise illuminated image. Increasing atomic number of the element gives rise to greater contrast of the image, making heavy metals such as silver and gold to stand out against organic compounds. This allows for observation of the atomic arrangement within particles making possible the identification of single crystals, twinning, phase differences, and grain boundaries. The self-assembly of nanoscale materials is of vital importance to the application of

metal particles to useful endeavors and will be discussed later. The assembly of the particles can be manipulated to suit a variety of needs; an electron microscope is pivotal in observing the details of which, an example is given in Figure 2.19 below.

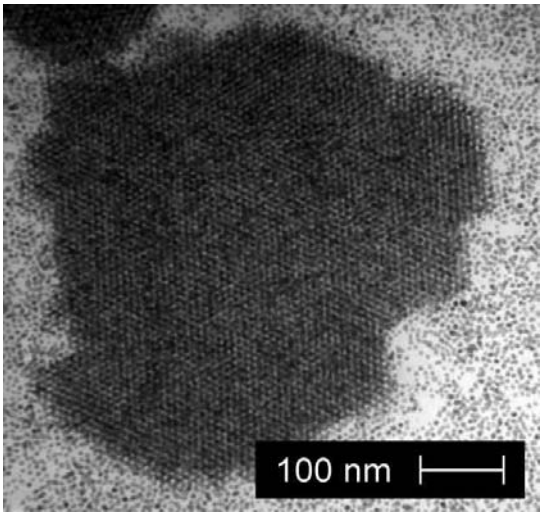

Figure 2.19 : Transmission electron microscope image of gold nanoparticles that have self assembled into a well-ordered superlattice.

In addition to providing visual information about the sample, additional spectroscopic attachments can be used to provide elemental and chemical data about individual particles while being viewed in the microscope. The combination of these techniques can be a very powerful tool to characterize nanoparticle samples.

2.3.2.2 Scanning electron microscopy

While the TEM can penetrate through samples, scanning electron microscopy scans a beam of electrons over a section of the sample and creates a topographical image of the surface of the particles. This instrument provides a 3-D image of the specimen and a clearer idea of the overall morphology of the sample. The resolution of an SEM is typically much more limited, with the best microscopes having the ability to resolve particles greater than 5 nm in diameter. Most instruments however can only discern differences in a sample that are at least 20 nm apart. The SEM is amenable to most of the spectroscopic attachments of the TEM allowing for chemical as well as structural information.

TEM and SEM instruments rely on a high vacuum system that can be difficult to maintain. Excess gas will deflect electrons and drastically reduce the intensity and

quality of spectra. This increases the cost of the instrument greatly, such that smaller institutes often will not have access to both microscopes, and often neither. SEM example is given in Figure 2.20.

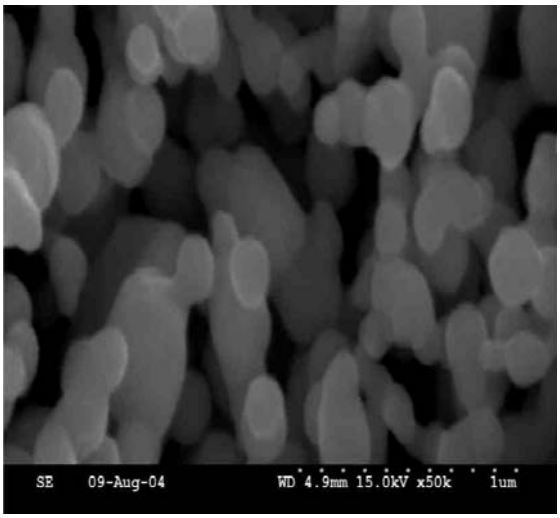

Figure 2.20: SEM Picture of silver nanosized powder displaying a very porous nature of the powder.

2.3.2.3 Atomic force microscopy

AFM instruments were first developed at the IBM laboratory in Zurich Switzerland. These instruments are typically far less expensive than TEM or SEM microscopes, but usually cannot provide as much sample information. AFM machines function by rastering the surface of a sample with a probe. The quality of the imaging is usually dependent on the sharpness of the probe itself (ideally ending in a single atom at the tip). The surface of the sample is constructed as a signal that is detected by electron tunneling across the space between the sample and the tip. By a feedback mechanism the tip can be set to a single potential and scanned across the sample surface. The z position of the tip is monitored and graphed as a 3-D topological map of the surface.

There are several benefits to AFM. Samples can be manipulated in a crude sense in the AFM by using the probe to physically push particles around or scratch the surface of the material, creating ordered structures mechanically on a length-scale of a few nanometers. It has no need of a high vacuum system as the samples can be tested in air, aqueous, or organic environments on the benchtop.

2.3.3 Applications of nanoparticles in the world

Nanoparticles are quickly going to find their way into our everyday lives. Metal nanoparticles in particular have a wonderful potential to improve the quality of life, and boost technology to a new level of excellence. One of the most apparent needs is the integration of nanoparticles into electrical components, further extending the power of today's computer systems. Nanoparticles are also being designed for sensors of unprecedented sensitivity unreachable from yesterday's micron sized devices. The potential of nanomaterials as catalysts and reactive centers is greatly amplified by the vast increase in the number of surface atoms in comparison to bulk counterparts. An example of this is the increased biological activity of silver metal nanoparticles against bacteria vs. the bulk metal [87-98].

2.3.3.1 Nano electronics

Despite their small size, above 1nm the products metal nanoparticles are composed of enough atoms to still behave as metals. The most exploitable property of this is that the particles have a plethora of electrons all at a very similar energy to one another and can be easily conducted or stored on a particle. In conjunction with the nanoparticles' incredibly small size this allows for the possibility of creating incredibly small electronic components. Quinn and coworkers have demonstrated the versatility of a nanoparticle as an electron storage center by observing 15 different oxidation states on a gold nanoparticle as electrons are stored or removed from the metal dot [87]. The most common preparation for nanoparticles leaves the metal sphere protected by a monolayer of a dodecane thiol molecule. This layer is insulating making each particle intrinsically a nanocapacitor where a small amount of energy can be stored.

The great difficulty has been found to not be the formation of these incredibly small electrical components, but in connecting them and their communication with one another. One ingenious method is the use of double stranded deoksiribonükleik asit (DNA) to crosslink the nanoparticles by functionalizing the nanoparticle itself with oglionucleotides that will selectively attach the particle to specific parts of the DNA strand. If impregnated with $[Ru(NH_3)_6]^{3+}$ the DNA strand provides a tunneling route for electrical currents [88]. An alternative method of creating a planned electronic

circuit was the use of aryl dithiols and dinitriles to connect metal nanoparticles to one another in a 2-D array. In this way the Andres group measured the conductance of several metal clusters with organic linkers with various lengths [89].

Metal nanoparticles can be integrated into media storage devices in ways other than by storage of electrons as well. Magnetic particles can also be created using some of the synthetic methods mentioned above. For example Ono *et al* created Mn-Pt ferromagnetic alloys for this purpose [90]. The major limitation of these materials is the ability to orient the nanoparticle to a certain value (N or S) and have it remain at that value at room temperature. Often times even at this temperature there is enough energy for the particles to rotate and move freely of their own. Another interesting route to a high memory density material, however read only, can be obtained by utilizing the bright optical absorption of the nanoparticles. Hodak formed core-shell alloys of gold/silver nanoparticles with a complex absorption [91]. These particles can quickly and easily be converted to alloys by irradiation of a laser. Careful writing on a 2D superlattice of these core shell particles could lead to huge information storage in exceptionally small areas [92].

2.3.3.2 Surface enhanced raman spectroscopy

A very interesting application has arisen recently from noble metal nanoparticles. This arises from a phenomenon discovered by Martin Fleischmann in 1974. He noticed an unusually large Raman signal from a pyridine molecule absorbed on a roughened silver electrode [93]. Attempts to study and enhance this behavior led scientists to find that this surface enhanced raman spectroscopy (SERS) effect only occurs near noble metal surfaces that have nanosized features. It is still not completely understood why, but the surface plasmon resonance effect displayed by the nanoparticles has an enormous enhancement on Raman signals. The increase is large enough to boost the sensitivity of the signal to 10^{16} times its normal operational limit. In fact single molecule detection has been observed for certain dye molecules absorbed on specially created silver surfaces. New sensors based on this type of SERS signals offer unbelievable increases in sensitivity for applications that including homeland security, as explosives, and toxins can be detected at miniscule levels. SERS sensors have made Raman spectroscopy a true compliment for IR spectroscopy allowing analysis of smaller quantities of materials.

2.3.3.3 Metal nanoparticles as biosensors

In a more straightforward use of the sensitivity of the optical response of the nanoparticles in relation to their environment is the use of silver nanoparticles as optical biosensors. By coating silver nanotriangles with biotin, Van Duyne and coworkers were able to detect very small amounts of streptavidin which would complex with the biotin and cause the electronic contribution of the ligand to the nanoparticle to change. Again the small size of these materials and large response to small amounts of stimuli make metal nanoparticles ideal sensors. There have been many studies into the use of nanoparticles as biosensors. Gold is typically the material chosen as it is the most chemically stable product available, and it can be functionalized with relative ease by thiol containing molecules. El-Sayed's group tried to create cancer cell detectors by coating gold nanoparticles with a receptor for a protein called an epidermal growth factor receptor [94]. Cancerous cells were found to display this protein much more extensively than normal cells. In a process first conducted by Chad Mirkin at Northwestern University, the color change of gold colloid between soluble particles and agglomerations is a very strong red to blue change. Gold nanoparticles coated with DNA base pairs will reversibly agglomerate when the complimentary DNA strand is entered into solution. This simple method has been shown to have amazing sensitivity and selectivity often recognizing the difference between DNA with a single different base pair [95]. This has even been carried out to the extent where colorimetric biosensors have been made to detect the presence of lead in ultra low concentrations [96].

2.3.3.4 Antimicrobial action of silver nanoparticles

Several research groups have looked into the potential for silver nanoparticles to be used as antimicrobial agents. Silver has long been known for its lethality to single celled organisms. It is hoped that the along with increased surface area nanoparticles of silver can be found to have increased action to pathogens. Nurcryst pharmaceuticals has already produced a burn wound dressing that is impregnated with silver nanoparticles that have proven superior in its ability to keep a burn wound clean and decreases the time to heal the wound itself [97]. Nanoparticulate silver may indeed find its way into a great many applications as the need for sterile surfaces arise.

2.3.3.5 Catalysts

The potential for nanomaterials as catalysts is possibly more tremendous than any physical property of the materials. The incredibly small size of the nanoparticles creates a high number of surface atoms, in fact up to 50% of the atoms may reside on the surface of the particle available for reaction. When coated with ligand molecules the surfaces that previously needed to be used as heterogeneous catalysts can now be incorporated into homogeneous systems that can then be precipitated from solution. Use of metal nanoparticles as a catalyst has already been tested for aiding solution phase chemistry, as shown by Yeh's group who reported large advances for the Heck reaction with a Au-Ag-Pt trimetallic particle [98]. Metal nanoparticles involved as catalysts for the cleavage of oxygen and hydrogen gas have been incorporated into electrodes for fuel cells, a scientific technology that may drastically change the way the world consumes energy.

3. EXPERIMENTAL WORK

3.1 Materials

Refined sunflower oil purchased from the market was used as receieved. Sunflower oil is semidrying oil and contains mainly oleic and linoleic acids bearing one and two double bonds on their chains, respectively. The average molecular weight of the sunflower oil, based on the ester value, was found to be 895 $g.mol^{-1}$. Toluene diisocyanate (TDI, 98%, Aldrich), silver nitrate ($AgNO_3$, 98%, Aldrich) and 2,2-dimethoxy-2-phenyl acetophenone (DMPA, Ciba Specialty Chemicals) were used without further purification. Monomers, styrene (St) and 2-hydroxyethyl methacrylate (HEMA) were purchased from Aldrich and passed through a basic alumina column to remove the inhibitor before use. 2,2'-Azoisobutyronitrile (AIBN, Fluka) was recrystallized from ethanol.

3.2 Equipment

3.2.1 Photoreactor

A Rayonet type photoreactor equipped with 16 Philips 8W / 06 lamps emitting light nominally at 350 nm was used.

3.2.2 Gel permeation chromatography (GPC)

Gel permeation chromatography analyses were performed with a set up consisting of a Waters 410 Differential Refractometer, a Waters 515 HPLC Pump and an apparatus equipped with three Waters ultrastyragel columns (HR series 4, 3, 2 narrow bore), with THF as the eluent at a flow rate of 0.3 mL/min. Molecular weights were calculated on the basis of a calibration curve recorded with monodisperse polystyrene standards.

3.2.3 Fourier transform infrared spectroscopy (FT-IR) analysis

FT-IR spectra were recorded on a Perkin Elmer FT-IR Spectrum One B spectrometer.

3.2.4 Thermal gravimetric analysis (TGA)

Perkin Elmer Diamond TG/DTA was used for TGA analysis. The measurements were done from +50 ºC to +1200 ºC with a heating rate of 20 ºC/min. The analysis was used to determine the solid content left when the polymer was heated up to 1200 ºC.

3.2.5 Dynamic mechanical analysis (DMA)

The Perkin Elmer was used to measure the oil based polymer and oil based polymer-silver nanocomposites. The material tested had dimensions of 0.18×10×40 mm. The material was heated from -10 ºC to +180 ºC with a heating rate 3 ºC/min. The applied frequency was 1 Hz.

3.2.6 Transmission electron microscopy

For preparation of TEM sample, thin film samples were prepared by cutting the cross-linked composite by using microtome apparatus. Then samples were placed on a thin copper grid covered by a plastic or carbon film that supports the sample to be viewed. The sample was ready for observing with TEM. JEOL JEM 1011 operated at 80 kV was used to conduct TEM observations.

3.3 Preparation Methods

3.3.1 Preparation of partial glyceride

Partial glyceride was prepared by glycerolysis reaction between triglyceride oil and glycerol. For the urethane oil preparation, the reactant ratio given by Stanton [99] was applied. Thus, 120 g of oil and 10.4 g of glycerol, (oil/glycerol, mol/mol:1.19), were placed into the reaction flask and heated. When the temperature reached to 218˚C, calcium hydroxide (0.1 wt% of the oil) was added as catalyst. The

temperature was then set at 232 ˚C and kept constant. At predetermined time intervals, samples were taken and poured into three-fold ethanol. Transesterification reaction was ended when the alcohol solution became clear. The reaction was continued for 1 h. The flask content was taken into diethyl ether and washed first with dilute sulphuric acid and then with distilled water to remove the catalyst and free glycerol. In order to understand that the glycerol was removed completely, the spot test based on selective oxidation of glycerol with periodic acid was applied to the washings [100]. The etheral solution was dried over Na_2SO_4 and the solvent was removed. The hydroxyl value of the dry and glycerol free sample was determined. The hydroxyl value is the number of mg. of potassium hydroxide required to neutralize the amount of acetic acid capable of combining by acetylation with 1g. of sample. For this determination acetic anhydride solution in prydine was used as acetylation agent [101].

3.3.2 Preparation of oil based macromonomer from partial glycerides

Preparation of oil based macromonomer, partial glyceride and HEMA were combined through urethane linkage by the reaction with TDI. The reactants (TDI, HEMA, and [OH] contributed by partial glyceride) were used in equimolar amounts and heated in dry xylene to 40-50 ˚C, and TDI was added slowly over a 30 min. period. Lead naphthenate as a 24 wt% solution in white spirit was added in the amount of 0,02 wt% of the oil portion. The temperature was set at 90-95 ˚C and reaction was continued for 4 h.

3.3.3 Preparation of oil based polymer silver nanocomposites by electron transfer reaction and thermally induced polymerization processes

Using electron transfer reaction and free radical polymerization processes a series of triglyceride oil based polymer/silver nanocomposites were successfully prepared. The whole process was divided into two simultaneous stages; (i) copolymerization of macromonomers obtained from partial glycerides with styrene and (ii) the reduction of silver nitrate to metallic silver nano particles with radicals stemming from the thermolysis of 2,2'-azoisobutyronitrile (AIBN). The conditions for the synthesis of the nanocomposite films are summarized in Table 3.1. Oil based macromonomer was first dissolved in styrene at a various macromonomer/styrene weight ratio to form a

homogeneous solution. Appropriate amount of silver nitrate was then added to this solution and mixed at room temperature until siver nitrate crystal were vanished. This directly indicates the uptake of silver nitrate by the macromonomer in the solution. After all the silver nitrate crystals disappeared, the radical initiator, AIBN was added and the content was stirred until it became clear (Stage A) in a manner similar to that described by Kim *et al* [25]. Then the film samples were prepared on glass plate by using Bird film applicator and subsequently placed in an oven maintained at 65˚C for 4 h to complete polymerization. At the end of the polymerization, cross-linked samples were further kept in an oven under vacuum. The remaining monomer, if any, was removed by treatment with methanol. In order to prevent the oxidization of silver nitrate by light, all processes were carried out in the dark.

Table 3.1 : Synthesis[a] recipe for oil based polymer composite (OBPC) containing silver nanoparticles.

Sample	Macromonomer (g)	Styrene (g)	AIBN (mol)x10^{-4}	$AgNO_3$ (mol)x10^{-4}
OBPC-1	1	2	1.81	1.77
OBPC-2	1	2	0.61	1.77
OBPC-3	1	3	0.61	1.77

[a]Polymerization was performed at 65˚C for 4 h.

3.3.4 Preparation of oil based polymer silver nanocomposites by electron transfer reaction and photochemically induced polymerization processes

In situ synthesis of oil based polymer/silver nanocomposites was prepared by using photoinduced free radical polymerization processes in which silver nanoparticles were formed by electron transfer reaction. An oil based macromonomer was prepared and then copolymerized with styrene in the presence of $AgNO_3$. Copolymerization was started with free radicals formed by photolysis of 2,2-dimethoxy-2-phenyl acetophenone and simultaneously silver nitrate was reduced to metallic silver in nanosize by electron transfer reaction. For the synthesis of the nanocomposite films, the same procedure applied as in the previous study was

carried out with the ingredient amounts given in Table 3.2.

Table 3.2 : Synthesis[a] of oil based polymer nanocomposite (OBPC) containing silver nanoparticles at room temperature for 4 h. at λ=350 nm.

Sample	Macromonomer (g)	Styrene (g)	DMPA (mol)x10^{-4}	$AgNO_3$ (mol)x10^{-4}
OBPC-A	1	3	1.17	2.34
OBPC-B	1	3	2.34	2.34
OBPC-C	1	3	4.68	2.34

[a]Photopolymerization was carried out at λ=350 nm for 4 h. Light intensity is 1.04 mW cm^{-2}.

Oil based macromonomer was first dissolved in styrene to form a homogeneous solution with a weight ratio of macromonomer/styrene is given in Table 3.2. Given amount of silver nitrate was then added and mixed with macromonomer/styrene mixture at room temperature. Although the silver nitrate salts did not dissolve, they did disperse in the hydrophobic monomer (styrene) and the crystals vanished while the mixture was being stirred. This directly indicates the uptake of silver nitrate by the macromonomer chains in the solution. After all the silver nitrate crystals were disappeared, the photoinitiator was added. The mixture was stirred until it became clear (Stage A). Then the film samples were prepared on glass plate by using Bird film applicator and subsequently placed in a photoreactor maintained at room temperature for 4 h to complete polymerization. Rayonet merry-go-round photoreactor was used to perform the polymerizations in which the sample was surrounded by a circle of 16 lamps emitting light nominally at 350 nm. The light intensities at the location of the photocuring sample were measured by a Delta Ohm model HD-9021 radiometer. At the end of the polymerization, cross-linked samples were further kept in an oven under vacuum to remove the free styrene monomer. The remaining monomer, if any, was removed by treatment with methanol.

3.3.5 Characterization of oil based macromonomer and polymer silver nanocomposite film

Molecular weights were determined using a Gel Permeation Chromatography (GPC) instrument equipped with a Waters styragel column (HR series 2, 3, 5E) with THF as the eluent at a flow rate of 0.3 mL min^{-1} and a Waters 410 Differential Refractometer detector. The structure of macromonomer was characterized by using fourier-transform infrared spectroscopy (recorded on a Perkin Elmer FT-IR Spectrum One B spectrometer).

The structures of the film samples were characterized by Transmission Electron Microscopy (TEM) JEOL JEM 1011 and Thermogravimetric analysis (TGA) was carried out with a thermogravimetric analyser (TA Instrument, TGA 2050). For the TEM measurements, thin film samples were prepared by cutting the cross-linked composite by using microtome apparatus. The film properties such as flexibility (according to the DIN 53 152), adhesion (according to the ASTM D 3359-90 Test method B.), rocker hardness, water resistance (according to the ASTM D 1647-89), alkali resistance (according to the ASTM D 1647-89), and acid resistance (according to the ASTM D 1647-89) were determined [102-104]. Film samples on the related substrates were prepared with the reaction content of Stage A. Then the film samples were placed in an oven and in a photoreactor to complete thermal polymerization and photopolymerization, respectively. For the flexibility and water resistance tests, tin plate panels were used as a substrate, while glass tubes were used for the alkaline and acid resistance tests, as explained in the related standard methods. In adhesion and hardness determinations, a Bird film applicator with 40 μm aperture was used for film application on glass plate. For other tests films are performed by dipping method.

For the examination of the antibacterial activity of the composites, inhibition zone test was applied to film samples with and without silver nanoparticles. The film samples were immersed into the water for 48 h at 20˚C before the test. The antibacterial properties were evaluated against Gram-positive (*Staphylococcus aureus*, ATCC 6538), Gram-negative bacteria (*Pseudomonas aeruginosa*, NCTC 6749), and spore forming (*Bacillus subtilis*, ATCC 9372) bacteria. All bacterial suspensions which previously adjusted to 0.5 McFarland turbidity (10^8 CFU/mL.)

were inoculated onto Mueller-Hinton agar and tests were performed according to described method [105-109]. The films were placed on inoculated agar plates, and incubation was performed at 37ºC for 24h .

4. RESULTS AND DISCUSSIONS

4.1 Synthesis of Oil Based Macromonomer from Partial Glycerides

Triglyceride oil based vinyl macromonomer were prepared by two successive steps. First, partial glycerides were obtained by glycerolysis reaction of triglyceride with glycerol as depicted in Figure 4.1. The hydroxyl and acid values (acid value, number of mg. of potassium hydroxide to neutralize the acids present in 1 g. of sample)of the partial glyceride were found to be 113 and 2.45, respectively.

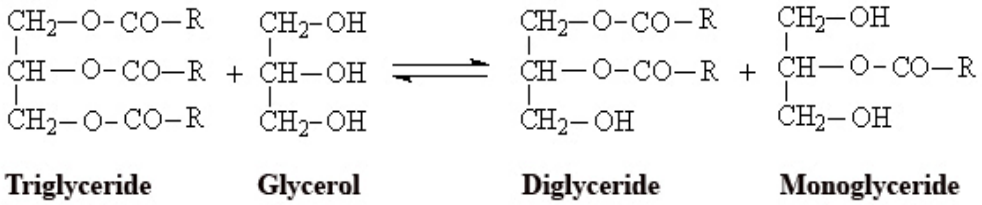

Figure 4.1 : Synthesis of partial glycerides.

Subsequently, these partial glycerides were combined with HEMA through urethane linkage by using TDI (Figure 4.2) in equivalent amount to total hydroxyl groups. The reaction between isocyanates and hydroxyl groups forming urethane linkage was monitored by FTIR. In the FTIR spectra of macromonomer (Figure 4.3) free isocyanate peak at 2265 cm^{-1} disappeared after 4 h indicating completion of the reaction. As illustrated in Figure 4.2, through the hydroxyl groups of mono- and di-glycerides polymerizable methacrylate double bonds were inserted into the structure. The unsaturated terminal groups are expected to act as cross-linker in the subsequent polymerization step. The number of average molecular weight of the macromonomer synthesized was determined by GPC and found to be 3280 with a polydispersity of 2.21. The observed relatively high polydispersity is expected since the obtained macromonomer is a mixture of various products formed from mono and diglycerides.

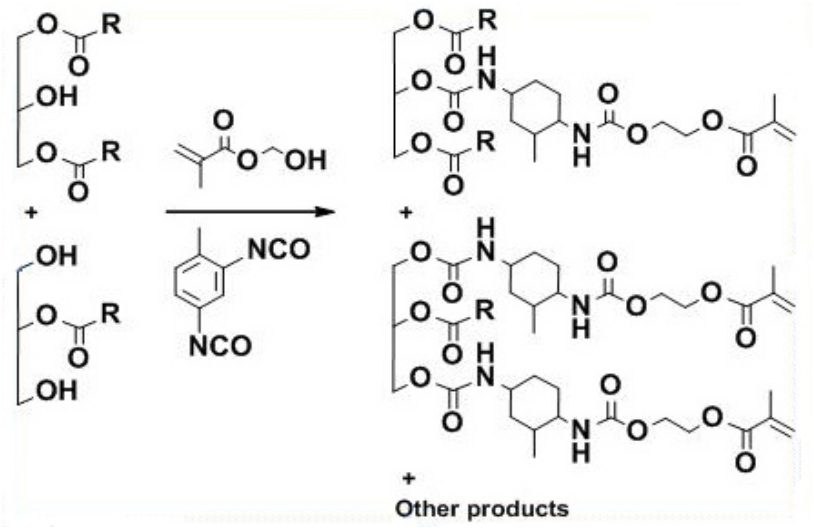

Figure 4.2 : Synthesis of partial glyceride macromonomers.

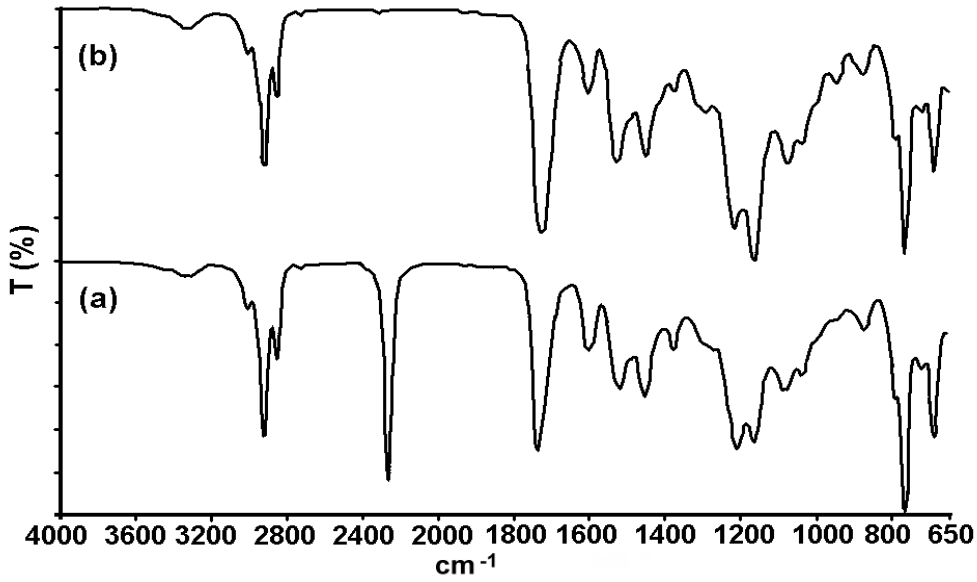

Figure 4.3 : FTIR spectra of TDI based reaction mixture (a) at the beginning (b) after 4 h final product.

4.2 *In situ* Synthesis of Oil Based Polymer Silver Nanocomposite Films by Thermally and Photochemically Induced Polymerization

In the polymerization of macromonomer with styrene the free radicals stemming from the thermolysis of AIBN and photolysis of DMPA initiate the polymerization, and at the same time, partly undergo electron transfer reaction with the silver salt present in the system. Thus, reduction to metallic silver and cross-linking polymerization occur simultaneously. The overall process for the *in situ* synthesis of oil based polymer/silver nanocomposite both thermally and photochemically ınduced polymerization are represented in Figure 4.4 and Figure 4.5.

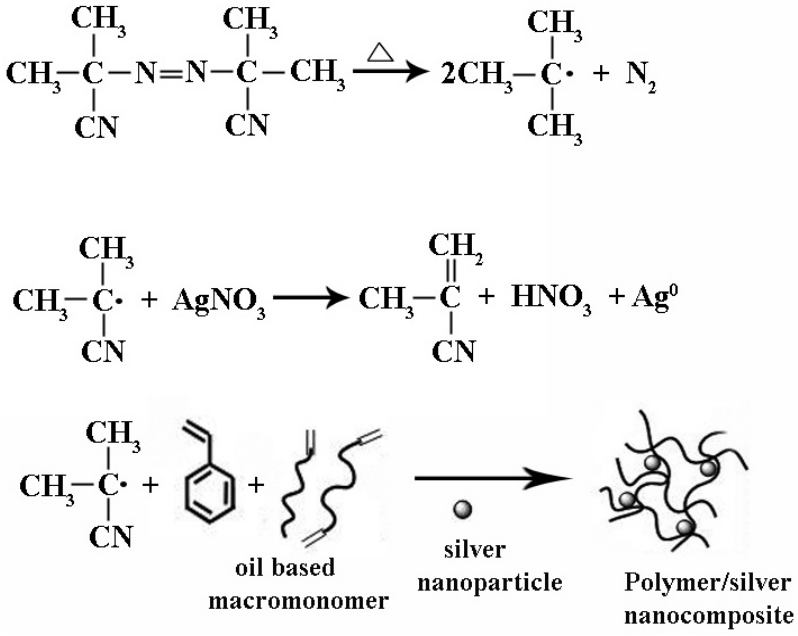

Figure 4.4 : *In situ* synthesis of triglyceride oil based polymer/silver nanocomposite by thermally induced polymerization.

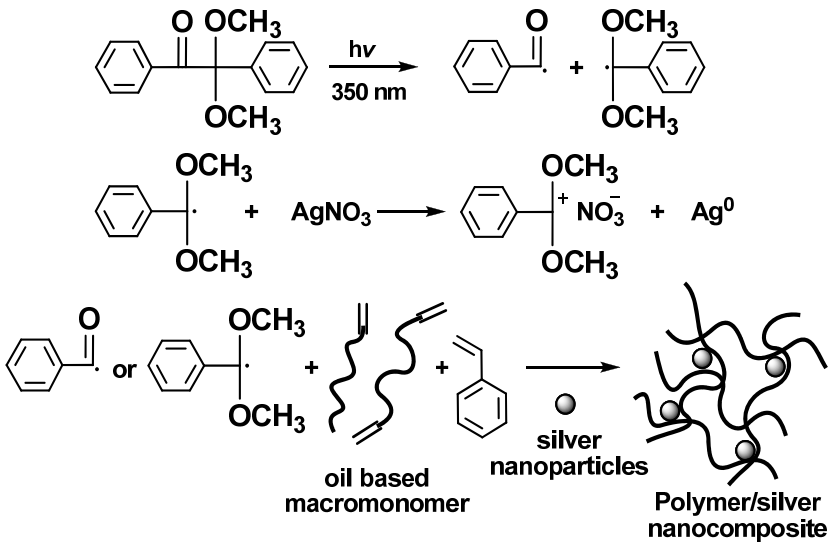

Figure 4.5 : *In situ* synthesis of triglyceride oil based polymer/silver nanocomposite by photochemically induced polymerization.

4.3. Characterization of Polymer Silver Nanocomposite Films

4.3.1 Transmission electron microscopy results

The oil silver nanocomposite samples were prepared by changing the amount of ingredients, see Table 3.1 and Table 3.2. All the composites prepared were transparent indicating the formation of silver particles in nanometer range size, which was also confirmed by TEM analysis. In Figure 4.6, bright field TEM micrographs for the composites prepared by using 1 wt % AIBN (based on macromer) and macromer/styrene weight ratio of 1:2 is reported. It can be seen that metallic particles are well dispersed with no significant macroscopic agglomerations. The particle size distribution is within the range of 13-26 nm. It should be noted that when the AIBN concentration was increased threefold, particle size increased the range being 20-40 nm. This indicates that the size of silver nanoparticles formed within the polymer matrix strongly depends on the concentration of radical initiator. At a higher AIBN concentration, a higher number of radicals are formed and consequently causes the formation of a greater number of silver nanoparticles which increases probability of their interaction resulting in aggregation. It is also interesting to note that, when the styrene content in the feed is increased, the hydrophobic domain increases which results in the formation silver nanopartciles with smaller size being in the range of 8-20 nm.

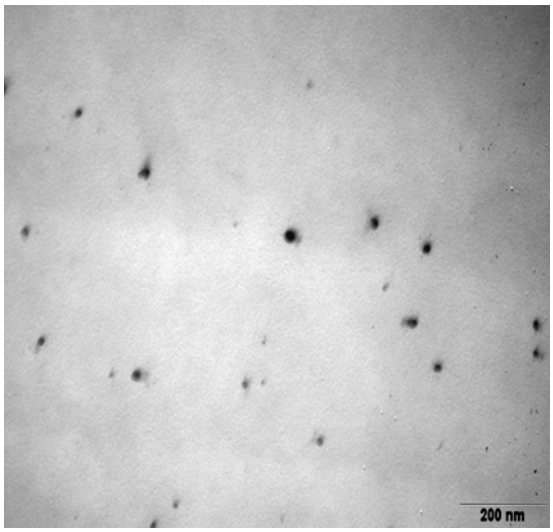

Figure 4.6 : TEM images of oil based polymer composite containing silver nanoparticles synthesized by using 1 wt. % of AIBN (based on macromer) and weight ratio of macromer/styrene 1:2.

In Figure 4.7, bright field TEM micrographs for the composites prepared by using various weight percentage of DMPA based on macromonomer/styrene mixture. TEM images of the composite films illustrated in Figure 4.7, show that nano-sized silver particles (8-50 nm) were dispersed in the polymer matrix. The size of silver nanoparticles increased from 8 nm to 50 nm as the weight percentage of DMPA in the macromonomer/styrene mixture was increased from 0.75 to 3. This indicates that the size of silver nanoparticles formed within the polymer matrix strongly depends on the concentration of photoinitiator. At higher DMPA concentration, a higher number of radicals are formed and consequently leads to aggregation of silver particles due to the higher probability of particle interaction with each other.

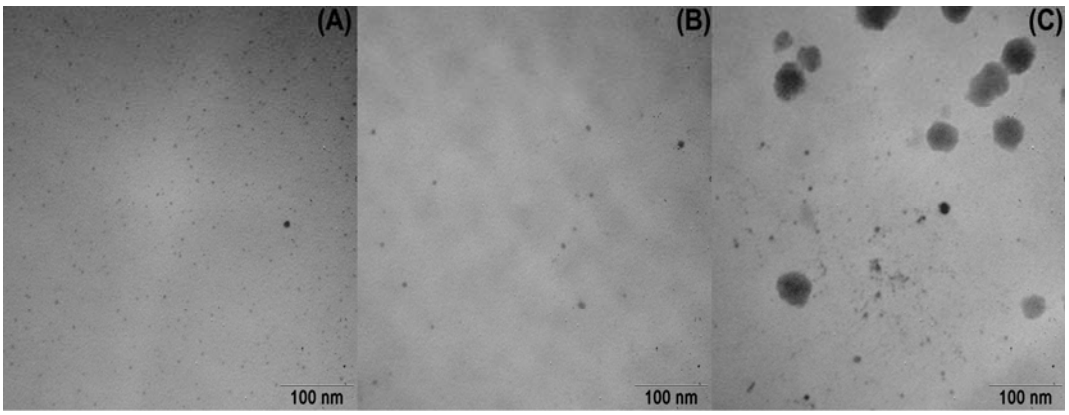

Figure 4.7 : TEM images of oil based polymer composite containing silver nanoparticles synthesized by using 0.75 wt. % of DMPA (A) 1.5 wt. % of DMPA (B) 3 wt. % of DMPA (C) (based on macromonomer / styrene mixture).

4.3.2 Thermogravimetric analysis results

Thermogravimetric analysis of the polymer composite film samples which produced thermally and photochemically induced polymerization, was also carried out and compared with that of the network formed under identical experimental conditions in the absence of silver nitrate (Figure 4.8 and Figure 4.9). Interestingly, the sample prepared without silver lost 98 % of its original weight at 480 °C whereas nanosized silver containing sample lost 88 % in Figure 4.8. In Figure 4.9, the sample prepared without silver lost 88 % of its original weight at 480 °C whereas nanosized silver containing sample lost 76 %. This implies that even very little amount of silver (1 %) nanoparticles gives an important thermal stability to degradation.

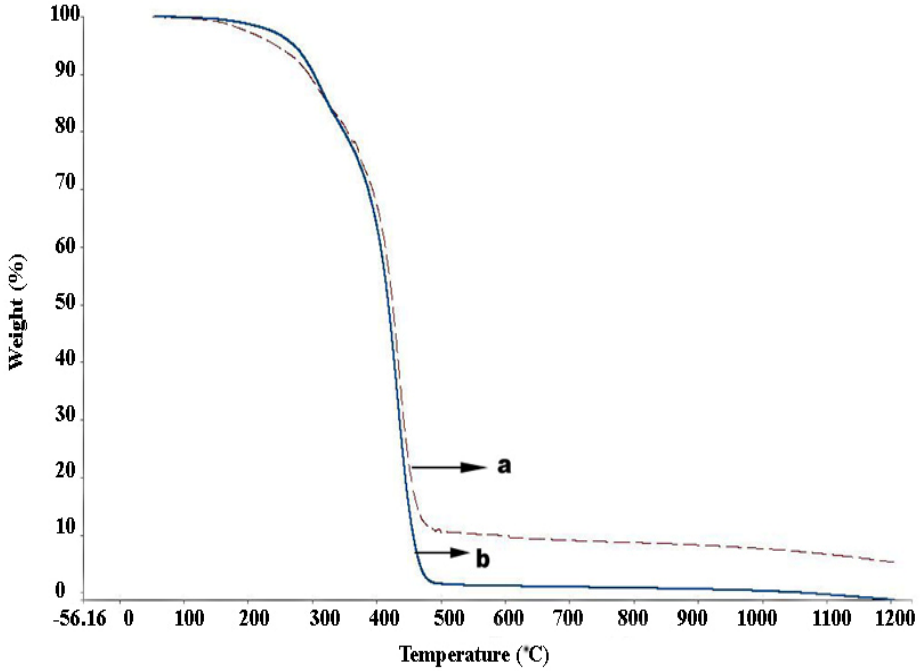

Figure 4.8 : TGA curves of (a) thermally induced oil based polymer nanocomposite and (b) styrenated oil by macromonomer method.

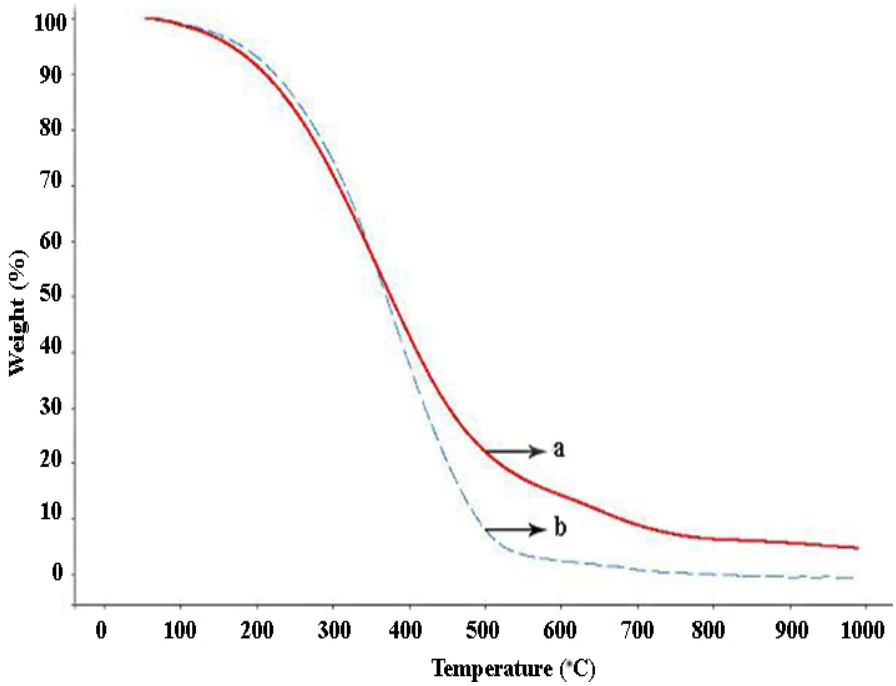

Figure 4.9 : TGA curves of (a) photochemically induced oil based polymer nanocomposite. and (b) styrenated oil by macromonomer method.

4.3.3 Dynamic mechanical analysis results

The DMA results of pure oil based polymer and oil based polymer-silver nanocomposites are shown in Figure 4.10. It shows the behavior of oil based polymer with and without silver nanoparticle. The pure oil based polymer starts to soften at -46 ºC measured by the onset value of tan delta. This the α transition of the polymer which means the glass transition temperature. The materials modulus values decrease very sharply as a consequence of the glass transition. Afterwards, the polymer comes to a rubbery linear region after the glass transition. The material continues to lose strength upon heating but the slope is less than the glass transition period. When the oil based polymer is reinforced with the silver the modulus values and glass transition temperatures (T_g=94 ºC) increase. The modulus values and glass transition temperatures of the nanocomposites are higher than the pure polymer at all temperatures except before the its glass transition temperature value. When we investigate the tan delta peaks of pure oil based polymer and oil based polymer-silver nanocomposite samples, it is observed that the tan delta peaks do shift significantly. This shows that the nanocomposites do alter Tg value of the pure oil based polymer.

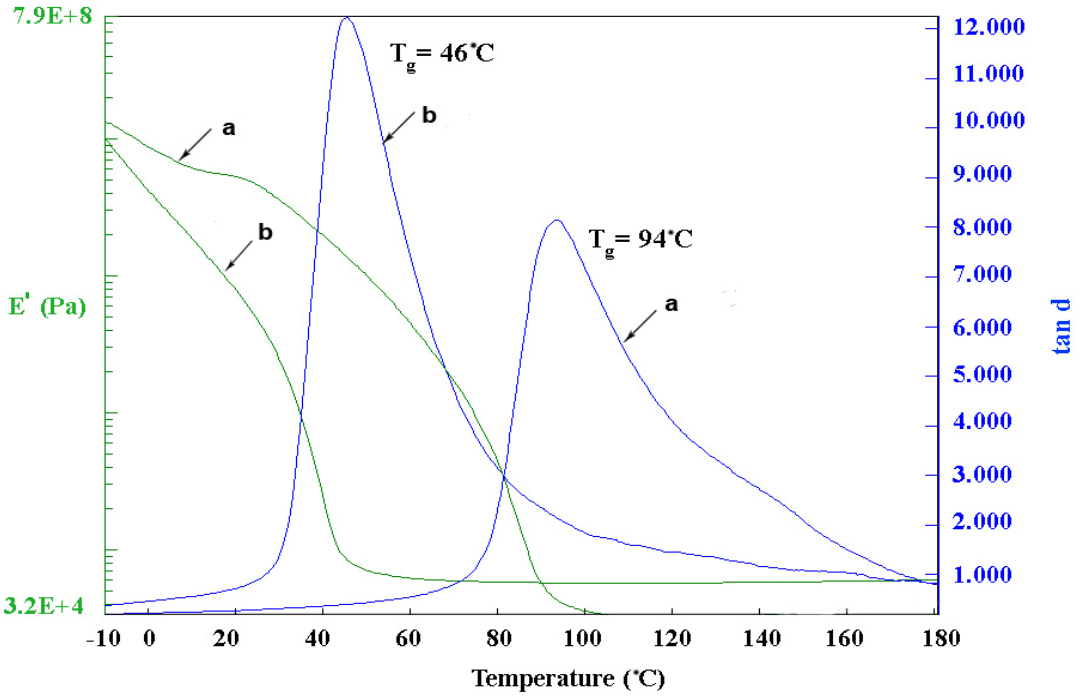

Figure 4.10 : DMA of (a) oil based polymer containing silver nanoparticle (b) pure oil based polymer

4.4 Film Properties of the Polymer-Siver Nanocomposite Films and Polymer Samples without Metal Particles

For their potential use as coating materials, film properties of the nanocomposite samples which produced by thermally and photochemically induced polymerization and polymer samples without metal particles were determined. The results obtained were collected in Table 4.1 and Table 4.2. As shown, composite and polymer samples showed good adhesion, flexibility, water, acid, and alkali resistances. Compared to classical styrenated oil, the samples with and without nano-sized silver showed better film properties.

Table 4.1 : Film properties of polymer films prepared by thermally induced polymerization at different conditions containing silver nanoparticles.

	Applied Test					
Sample	**Flexibility[a]**	**Adhesion[b]**	**Hardness**	**Acid Resistance[c]**	**Alkali Resistance[d]**	**Water Resistance**
OBPC-1[e]	2 mm	5B	14	no change	75 min pp.	no change
SO-M[f]	2 mm	5B	6	no change	53 min pp.	no change
SO-C[g]	2 mm	5B	------	no change	31 min pp.	5 min

[a] The diameter of cylinder which caused no crack on the film
[b] Test method B was applied
[c] Test was carried out at 25 ^{o}C with 9 % H_2SO_4 solution
[d] Test was carried out at 25 0C with 3 % NaOH solution, pp = partial peeling
[e] Oil based polymer composite with silver nanoparticles (see Table 3.1. for the details)
[f] Styrenated oil prepared by macromonomer method [110].
[g] Styrenated oil prepared by classical method [111].

Table 4.2 : Film properties of polymer films prepared by photochemically induced polymerization at different conditions containing silver nanoparticles.

Applied Test						
Sample	**Flexibility**[a]	**Adhesion**[b]	**Hardness**	**Acid Resistance**[c]	**Alkali Resistance**[d]	**Water Resistance**
OBPC-B[e]	2 mm	5B	8	no change	94 min pp	no change
SO-M[f]	2 mm	5B	2	no change	45 min pp	no change
SO-C[g]	2 mm	5B	------	no change	31 min pp	5 min

[a] The diameter of cylinder which caused no crack on the film.
[b] Test method B was applied.
[c] Test was carried out at 25 ^{o}C with 9 % H_2SO_4 solution.
[d] Test was carried out at 25 ^{o}C with 3 % NaOH solution, pp = partial peeling
[e] Oil based polymer nanocomposite with silver nanoparticles (see Table 3.2. for the details)
[f] Styrenated oil prepared by macromonomer method [110].
[g] Styrenated oil prepared by classical method [111].

4.5 Antibacterial Properties of Polymer Silver Nanocomposite Films and Polymer Samples without Metal Particles

The obtained polymer nanocomposite film samples and polymer samples without metal particles which produced by thermally induced (Figure 4.10) and photochemically induced (Figure 4.11) polymerization were also examined in view of surface coating material with antibacterial effect against Gram-positive, Gram-negative, and Spore forming bacteria. It was demonstrated that the composite film sample had good antibacterial effect against Gram-positive (*S. aureus*), Gram-negative (*P. aeruginosa*), and spore forming (*B. subtilis*) bacteria as shown in Figure 4.11 and Figure 4.12. All kind of bacteria were killed and an inhibition zones were formed due to the antibacterial effect of the silver in the surrounding of the film samples. On the other hand, without silver no inhibition zone was detected. Additionally, after removing the silver composite films, incubation was continued for 24 h. at 37°C. At the end of this period, there was no bacterial growth indicating that the composite film has killing effect rather than growth inhibition.

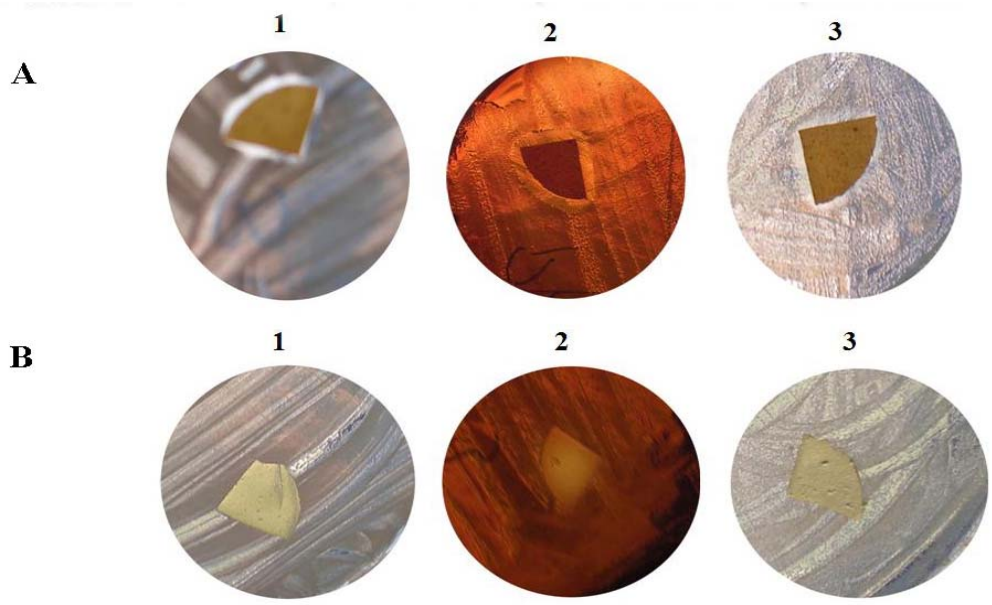

Figure 4.11 : Film samples prepared by thermally induced polymerization. Photographs showing zone of inhibition of the films prepared with 1 wt % of $AgNO_3$ (A) and without $AgNO_3$ (B): (1) *B. subtilis*, (2) *P. aeruginosa*, (3) *S. aureus*.

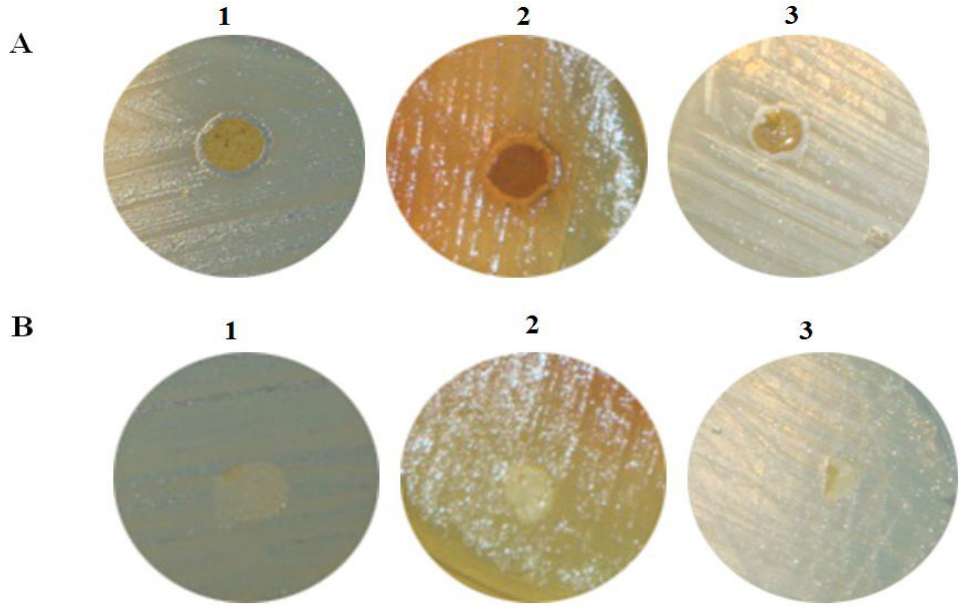

Figure 4.12 : Film samples prepared by photochemically induced polymerization. Photographs showing zone of inhibition of the films prepared with 1 wt % of $AgNO_3$ (A) and without $AgNO_3$ (B): (1) *B. subtilis*, (2) *P. aeruginosa*, (3) *S. aureus*.

5. CONCLUSION

In conclusion, *in situ* synthesis of triglyceride oil based polymer/silver nanocomposite was achieved by thermally induced and photochemically induced polymerization processes in which silver nanoparticles were formed by electron transfer reaction. It is known that one of the prominent ways to control size of nanoparticle and morphology is to employ functional polymeric nanostructures with well-defined interfaces. These interfaces can be generated via hydrophobic–hydrophilic microphase separation. In this study, hydrophilic and hydrophobic domains of the polymer are provided by the presence of oil portion (partial glyceride) and styrene segments in the structure, respectively. In the thermally induced polymerization and photoinitiated polymerization, while some of the radicals formed from the free radical initiator, AIBN and the photoinitiator, DMPA, induce copolymerization of the macromonomer with styrene, the other portion of the radicals involves electron transfer reaction to produce metallic silver nanoparticles. However, preparation of similar nanocomposites by photochemical means are now in progress. It is well known [112] that certain photoinitiators like DMPA generate free radicals with better electron donating properties and it is expected that these radicals may reduce silver salt more readily than those generated from AIBN.

The composites obtained in thermally induced and photochemically induced polymerization processeses contain homogenously distributed silver nanoparticles in the network without macroscopic agglomeration and exhibit good film as organic coating with antibacterial properties. It should also be emphasized that the importance of this study is closely related to the components of the network structure. The precursor triglyceride oil is obtained from renewable agricultural sources. Recently, the use of renewable sources in the preparation of various industrial materials has been revitalized because of the environmental concerns. Natural oils consisting predominantly of triglycerides are considered to be the most important class of renewable sources. In this context, we reported various

conceptually different strategies to synthesize polymers from triglyceride oils [113-115] and compared with the conventional methods [116]. Previously, amphiphilic block copolymers were used as templates for the preparation of inorganic nanoparticles [117-119]. However, amphiphilic block copolymers are very expensive materials and can only be obtained using extremely complicated synthetic processes. In the present study, a novel strategy was applied to synthesize nanocomposites from triglyceride oil based polymer exhibiting an amphiphilic characteristic to facilitate the formation of nanoparticles. This way, shortcomings associated with the high cost and complicated experimental procedures for the preparation of block copolymers were overcome.

REFERENCES

[1] **Okamoto, M., Morita, S., Taguchi, H., Kim, Y. H., Kotaka, T. and Tateyama, H.**, 2000, Synthesis and structure of smectic clay/poly(methyl methacrylate) and clay/polystyrene nanocomposites via in situ ıntercalative polymerization, *Polymer*, **41**, 3887-3890.

[2] **Ramos, J., Millan, A. and Palacio, F.**, 2000, Production of magnetic nanoparticles in a polyvinylpyridine matrix, *Polymer*, **41**, 8461-8464.

[3] **Zhu, Z. K., Yin, J., Cao, F., Shang, X. Y. and Lu, Q. H.**, 2000, Photosensitive polyimide/silica hybrids, *Advanced Materials*, **12**, 1055-1057.

[4] **Hatchett, D. W., Josowicz, M., Janata, J. and Baer, D. R.**, 1999, Electrochemical formation of au clusters in polyaniline, *Chemistry of Materials*, **11**, 2989-2994.

[5] **Chen, T. K., Tien, Y. I. and Wei, K. H.**, 2000, Synthesis and characterization of novel segmented polyurethane/clay nanocomposites, *Polymer*, **41**, 1345-1353.

[6] **Mukherjee, M., Datta, A. and Chakravorty, D.**, 1994, Electrical-resistivity of nanocrystalline Pbs grown in a polymer matrix, *Applied Physics Letters*, **64**, 1159-1161.

[7] **Forster, S. and Antonietti, M.**, 1998, Amphiphilic Block Copolymers in Structure-Controlled Nanomaterial Hybrids, *Advanced Materials*, **10**, 195-196.

[8] **Mayer, A. B. R.**, 2001, Colloidal metal nanoparticles dispersed in amphiphilic polymers, *Polymers for Advanced Technologies*, **12**, 96-106.

[9] **Beecroft, L. L. and Ober, C. K.**, 1997, Nanocomposite Materials for Optical Applications, *Chemistry of Materials*, **9**, 1302-1317.

[10] **Caseri, W.**, 2000, Nanocomposites of polymers and metals or semiconductors: historical background and optical properties, *Macromolecular Rapid Communications*, **21**, 705-722.

[11] **Gangopadhyay, R. and De, A.**, 2000, Conducting Polymer Nanocomposites: A Brief Overview, *Chemistry of Materials*, **12**, 608-622.

[12] **Spatz, J. P., Roescher, A. and Moller, M.**, 1996, Gold nanoparticles in micellar poly(styrene)-b-poly(ethylene oxide) films-size and ınterparticle distance control in monoparticulate films, *Advanced Materials*, **8**, 337-340.

[13] **Kane, R. S., Cohen, R. E. and Silbey, R.**, 1996, Synthesis of Pbs nanoclusters within block copolymer nanoreactors, *Chemistry of Materials*, **8**, 1919-1924.

[14] **Ghosh, K. and Maiti, S. N.**, 1996, Mechanical properties of silver-powder-filled polypropylene composites, *Journal of Applied Polymer Science*, **60**, 323-331.

[15] **Zhang, Z. P., Zhang, L. D., Wang, S. X., Chen, W. and Lei, Y.**, 2001, A convenient route to polyacrylonitrile/silver nanoparticle composite by simultaneous polymerization-reduction approach, *Polymer*, **42**, 8315-8318.

[16] **Hedden, R. C., Bauer, B. J., Smith, A. P., Grohn, F. and Amis, E.**, 2002, Templating of ınorganic nanoparticles by pamam/peg dendrimer-star polymers, *Polymer*, **43**, 5473-5481.

[17] **Bradley, J. S.**, 1994, *Clusters and Colloids from Theory to Applications*, Ed. Schmid D, Wiley-VCH, Weinheim, New York, 459-465.

[18] **Bronstein, L. M., Valetsky, P. M., Antonietti, M.,**, 1998, *Nanoparticles and Nanostructured Films: Preparation, Characterization and Applications,* Ed. Fendler J, Wiley-VCH, Weinheim, New York, 145-150.

[19] **Hirai, H., Toshima, N.,** , 1985, *Tailored Metal Catalysts*, Ed. Iwasawa Y, Reidel Publishing Company, Dordrecht, 121-135.

[20] **Klabunde, K. J., Efner, H. F., Murdock, T. O. and Ropple, R.**, 1976, Solvated nickel atoms and their free cluster formation in organic media, *Journal of the American Chemical Society*, **98**, 1021.

[21] **Clay, R. T. and Cohen, R. E.**, 1995, Synthesis of metal nanoclusters within microphase-separated diblock copolymers, *Supramolecular Science*, **2**, 183-186.

[22] **Clay, R.T. and Cohen, R.E.**, 1997, Synthesis of metal nanoclusters within microphase-separated diblock copolymers: ICP-AES analysis of metal ion uptake, *Supramolecular Science*, **2**, 113-115.

[23] **Huang, C. J., Yen, C. C. and Chang, T. C.**, 1991, Studies on the preparation and properties of conductive polymers: Metallized polymer-films by retroplating out, *Journal of Applied Polymer Science*, **42**, 2237-2245.

[24] **Gotoh, Y., Igarashi, R., Ohkoshi, Y., Nagura, M., Akamatsu, K. and Deki, S.**, 2000, Preparation and structure of copper nanoparticle/poly(acrylic acid) composite films, *Journal of Materials Chemistry*, **10**, 2548-2552.

[25] **Kim, J. Y., Shin, D. H., and Ihn, K. J.**, 2005, Synthesis of poly(urethane acrylate-co-styrene) films containing silver nanoparticles by a simultaneous copolymerization/in situ electron transfer reaction, *Macromolecular Chemistry and Physics*, **206**, 794-801.

[26] **Gunstone, F.**, 1996, *Fatty Acid and Lipid Chemistry*, Chapman and Hall, New York, 37-39.

[27] **Liu, K.**, 1997, *Soybeans: Chemistry, Technology, and Utilization,* Chapman and Hall, New York 218-226.

[28] **La Scala, J. J.**, 2002, The Effects of Triglyceride Structure on the Properties of Plant Oil-Based Resins, *Ph.D. Thesis,* University of Delaware, Delaware.

[29] **Motawie, A. M. and Sadek, E. M.**, 1998, Adhesives and coatings based on poly(vinyl acetal)s*, Journal of Applied Polymer Science*, **70**, 1769-1777.

[30] **Motawie, A. M., Hassan, E. A., Manieh, A. A., Aboulfetouh, M. E. and Eldin, A. F.**, 1995, Some epoxidized polyurethane and polyester resins based on linseed oil*, Journal of Applied Polymer Science*, **55**, 1725-1732.

[31] **Likavec, W. R. and Bradley, C. R.**, 1999, Ultraviolet and electron beam radiation curable fluorescent printing ink concentrates and printing inks*, U.S. Patent,* No: 5866628 dated 05.02.1999.

[32] **Pryde, E. H.,** 1979, Fats and oils as chemical intermediates: Present and future uses, *Journal of the American Oil Chemical Society*, **56,** 849-853.

[33] **Frischinger, I. and Dirlikov, S.**, 1991, Toughening of epoxy-resins by epoxidized vegetable-oils*, Polymer Communications*, **32**, 536-537.

[34] **Frischinger, I. and Dirlikov, S.**, 1994, Interpenetrating polymer networks*, Advances in Chemistry Series*, **239,** 552-554.

[35] **Mustata, F., Bicu, I. and Cascaval, C. N.**, 1997, Rheological and thermal behaviour of an epoxy resin modified with reactive diluents*, Journal of Polymer Engineering*, **17**, 491-506.

[36] **Rosch, J. and Mulhaupt, R.**, 1993, Polymers from renewable resources: polyester resins and blends and blends based upon anhydride-cured epoxidized soybeanoil*, Polymer Bulletin*, **31**, 679-685.

[37] **Barrett, L. W., Sperling, L. H. and Murphy, C. J.,** 1993, Naturally functionalized triglyceride oils in ınterpenetrating polymer networks*, Journal of the American Oil Chemical Society*, **70**, 523-534.

[38] **Devia, N., Manson, J. A., Sperling, L. H. and Conde, A.**, 1979, Simultaneous ınterpenetrating networks based on castor-oil elastomers and polystyrene: Stress-strain and ımpact loading behavior*, Polymer Engineering and Science*, **19**, 878-882.

[39] **Devia, N., Manson, J. A., Sperling, L. H. and Conde, A.**, 1979, Simultaneous Interpenetrating networks based on castor-oil elastomers and polystyrene: Morphology and glass-transition behavior*, Polymer Engineering and Science*, **19**, 869-877.

[40] **Devia, N., Manson, J. A., Sperling, L. H. and Conde, A.**, 1979, Simultaneous ınterpenetrating networks based on castor-oil elastomers and polystyrene: Synthesis and systems characteristics, *Macromolecules*, **12**, 360-369.

[41] **Li, F., Marks, D. W., Larock, R. C. and Otaigbe, J. U.**, 2000, Fish oil thermosetting polymers: Synthesis, structure, properties and their relationships, *Polymer*, **41**, 7925-7939.

[42] **Li, F., Larock, R. C. and Otaigbe, J. U.**, 2000, Fish Oil Thermosetting polymers: Creep and recovery behavior, *Polymer*, **41**, 4849-4862.

[43] **Li, F., and Larock, R. C.**, 2000, Thermosetting polymers from cationic copolymerization of tung oil: synthesis and characterization, *Journal of Applied Polymer Science*, **78**, 1044-1056.

[44] **Li, F. and Larock, R C.**, 2000, New Soybean oil-styrene-divinylbenzene thermosetting copolymers: Dynamic mechanical properties, *Journal of Polymer Science Part B: Polymer Physics*, **38**, 2721-2738.

[45] **Wool, R. P., Kusefoglu, S. H., Palmese, G. R., Zhao, R. and Khot, S. N.**, 2000, High modulus polymers and composites from plant oils, *U.S. Patent,* No: 6,121,398 dated 19.09.2000.

[46] **Rangarajan, B., Havey, A., Grulke, E. A., and Culnan, P. D.**, 1995, Kinetic parameters of a two-phase model for in situ epoxidation of soybean oil, *Journal of American Oil Chemical Society*, **72**, 1161-1169.

[47] **Zaher, F. A., El-Malla, M. H. and El-Hefnawy, M. M.**, 1989, Kinetics of oxirane cleavage in epoxidized soybean oil, *Journal of American Oil Chemical Society*, **66**, 698-700.

[48] **Sonntag, N. O. V.**, 1982, Glycerolysis of fats and methyl esters-status review and critique, *Journal of American Oil Chemical Society*, **59**, 795-802.

[49] **Swern, D.**, 1979, Bailey's Industrial Oil and Fat Products, Fourth edition, Vol. 1, John Wiley and Sons, New York, 159-166.

[50] **Cain, F. W., Kuin, A. J., Cynthia, P. A. and Quinlan, P. T.**, 1995, Fat blends containing diglycerides, *U.S. Patent,* No: 5,912,042 dated 09.06.1995.

[51] **Micciche, F.**, 2005, The Combination of Ascorbic Acid Derivatives/Iron Salts as Catalysy for the Oxidative Drying of Alkyd Based Paints, *Ph.D. Thesis*, Technische Universiteit, Eindhoven

[52] **Porter, M. A., Funk, M. O. and Isaac, R.**, 1975, Free radical cyclization of unsaturated hydroperoxides, *Journal of the American Chemical Society*, **97**, 1281-1282.

[53] **Mallegol, J., Lemaire, J. and Gardette, J. L.**, 2000, Drier ınfluence on the curing of linseed oil, *Progress in Organic Coatings*, **39**, 107-113.

[54] **Stenberg, C., Svensson, M. and Johansson, M.**, 2005, Study of the drying of linseed oils with different fatty acid patterns using rtir-spectroscopy and chemiluminescence, *Industrial Crops and Products*, **21**, 263-272.

[55] **Thames, S. F., Yu, H. B., Schuman, T. P. and Wang, M. D.**, 1996, Acrylated lesquerella oil in ultraviolet cured coatings, *Progress in Organic Coatings*, **28**, 299-305.

[56] **Hageman, H. J.**, 1985, Photoinitiators for free-radical polymerization, *Progress in Organic Coatings*, **13**, 123-150.

[57] **Monroe, B. M. and Weed, G. C.**, 1993, Photoinitiators for free-radical-ınitiated photoimaging systems, *Chemical Reviews*, **93**, 435-448.

[58] **Thames, S. F. and Yu, H.**, 1999, Cationic uv-cured coatings of epoxide-containing vegetable oils, *Surface and Coatings Technology*, **115**, 208-214.

[59] **Bradley, G.**, 1998, *Photoinitiators for Free Radical Cationic and Anionic Photopolymerization*, Second edition, John Wiley and Sons Publishers, Inc., New York, 329.

[60] **Crivello, J.V., Dietliker, K., and Bradley, G.**, 1999, *Photoinitiators for Free Radical Cationic and Anionic Photopolymerisation*, Second edition. John Wiley and Sons Publishers, Inc., Chichester, 266-268.

[61] **Nicolais, L. and Carotenuto, G.**, 2005, *Metal-Polymer Nanocomposites*, John Wiley and Sons Publishers, Inc., New Jersey, 155-157.

[62] **Sanchez, C., Soler I. G., Ribot, F., Lalot, T., Mayer, C. R. and Cabuil, V.**, 2001, Designed hybrid organic-ınorganic nanocomposites from functional nanobuilding blocks, *Chemistry of Materials*, **13**, 3061-3083.

[63] **Sankaran, V., Cummins, C. C., Schrock, R. R., Cohen, R. E. and Silbey, R. J.**, 1990, Small lead sulfide (Pbs) clusters prepared via romp block copolymer technology, *Journal of the American Chemical Society*, **112**, 6858-6859.

[64] **Ellsworth, M. W. and Gin, D. L.**, 1999, Recent advances in the design and synthesis of polymer-ınorganic nanocomposites, *Polymer News*, **24**, 331-341.

[65] **Turkevich, J., Stevenson, P. S. and Hillier, J.**, 1951, Study of the nucleation and growth processes in the synthesis of colloidal gold, *Discussions of the Faraday Society*, **11**, 55.

[66] **Van Hyning, D. L., Klemperer, W. G. and Zukoski, C. F.**, 2001, Silver nanoparticle formation: predictions and verification of the aggregative growth model, *Langmuir*, **17**, 3128-3135.

[67] **Van Hyning, D. L. and Zukoski, C. F.**, 1998, Formation mechanisms and aggregation behavior of borohydride reduced silver particles, *Langmuir*, **14**, 7034-7046.

[68] **Tan, Y., Jiang, L., Li, T. and Zhu, D.**, 2002, One dimensional aggregates of silver nanoparticles ınduced by the stabilizer 2-mercaptobenzimidazole, *Journal of Physical Chemistry B*, **106**, 3131-3138.

[69] **Leopokld, N. and Lendl, B.**, 2003, A new method for fast preparation of highly surface-enhanced raman scattering: Active silver colloids at room temperature by reduction of silver nitrate with hydroxylamine hydrochloride, *Journal of Physical Chemistry B*, **107**, 5723-5727.

[70] **Raveendran, P., Fu, J. and Wallen, S. L.**, 2003, Completely green synthesis and stabilization of metal nanoparticles, *Journal of the American Chemical Society*, **125**, 13940-13941.

[71] **Kim, F., Connor, S., Song, H., Kuykendall, T. and Yang, P.**, 2004, Platonic gold nanocrystals, *Angewandte Chemie*, **43**, 3673-3677.

[72] **Hiramatsu, H. and Osterloh, F. E.**, 2004, Simple large-scale synthesis of nearly monodisperse gold and silver nanoparticles with adjustable sizes and with exchangeable surfactants, *Chemistry of Materials*, **16**, 2509.

[73] **Bunge, S. D., Boyle, T. J. and Headley, T. J.**, 2003, Synthesis of metal nanoparticles from mesityl precursors, *Nano Letters*, **3**, 901-905.

[74] **Stoeva, S. I., Prasad, B. L. V., Uma, S., Stoimenov, P. K., Zaikovski, V., Sorensen, C. M. and Klabunde, K. J.**, 2003, Face-centered cubic and hexagonal closed-packed nanocrystal superlattices of gold nanoparticles prepared by different methods, *Journal of Physıcal Chemıstry B*, **107**, 7441-7448.

[75] **Ohde, H., Hunt, F. and Wai, C. M.**, 2001, Synthesis of silver and copper nanoparticles in a water in supercritical carbondioxide microemulsion, *Chemistry of Materials*, **13**, 4130-4135.

[76] **Choy, K. L.**, 2000, *Handbook of Nanostructured Materials and Nanotechnology*, Volume 1, Academic Press, San Diego, 533.

[77] **Stoeva, S. I., Klabunde, K. J., Sorensen, C. M., and Dragieva, I.**, 2002, Gram-scale synthesis of monodisperse gold colloids by the solvated metal atom dispersion method and digestive ripening and their organization into two- and three-dimensional structures, *Journal of the American Chemical Society*, **124**, 2305.

[78] **Smetana, A. B. and Klabunde, K. J.,** 2005, The synthesis of spherical silver nanoparticles with various ligands and their properties, *Journal of Colloid and Interface Science*, **284**, 521-526.

[79] **Lin, X. M., Sorensen, C. M. and Klabunde, K. J.**, 1999, Ligand ınduced gold nanocrystal superlattice formation in colloidal solution, *Chemistry of Materials*, **11**, 198.

[80] **Zhang, J., Han, B., Liu, M., Liu, D., Dong, Z., Liu, J., Li, D., Wang, J., Dong, B., Zhao, H. and Rong, L.**, 2003, Ultrasonication-ınduced formation of silver nanofibers in reverse micelles and small-angle x-ray scattering studies, *Journal of Physical Chemistry B*, **107**, 3679-3683.

[81] **Mizukosi, Y., Okitsu, K., Maeda, Y., Yamamoto, T. A., Oshima, R. and Nagata, Y.**, 1997, Sonochemical preparation of bimetallic nanoparticles of gold/palladium in aqueous solution, *Journal Of Physical Chemistry B*, **101**, 7033-7036.

[82] **Gao, F., Lu, Q. and Komarneni, S.**, 2005, Interface reaction for the self-assembly of silver nanocrystals under microwave-assisted solvothermal conditions, *Chemistry of Materials*, **17**, 856-860.

[83] **Harpeness, R. and Gedanken, A.**, 2004, Microwave synthesis of core-shell gold/palladium bimetallic nanoparticles, *Langmuir* **20**, 3431-3434.

[84] **Mallick, K., Wang, Z. L. and Pal, T.**, 2001, Seed-mediated successive growth of gold particles accomplished by uv ırradiation: a photochemical approach for size-controlled synthesis, *Journal of Photochemistry and Photobiology A*, **140**, 75-80.

[85] **Eustis, S., Hsu, H. Y. and El-Sayed, M. A.**, 2005, Gold nanoparticle formation from photochemical reduction of Au^{3+} by continuous excitation in colloidial solutions: A proposed molecular mechanism, *Journal of Physical Chemistry B*, **109**, 4811-4815.

[86] **Rongchao, J., Cao, Y., Mirkin, C. A., Kelly, K. L., Schatz, G. C. and Zheng, J. G.**, 2001, Photoinduced conversion of silver nanospheres to nanoprisms, *Science*, **294**, 1901-1903.

[87] **Quinn, B. M., Liljeroth, P., Ruiz, V., Laaksonen, T. and Kontturi, K.**, 2003, Electrochemical resolution of 15 oxidation states for monolayer protected gold nanoparticles, *Journal of the American Chemical Society*, **125**, 6644-6645.

[88] **Willner, I., Patolsky F. and Wasserman, J.**, 2001, Photoelectrochemistry with controlled dna-cross-linked cds nanoparticle arrays, *Angewandte Chemie International Edition*, **40**, 1861.

[89] **Andres, R. P., Bielefeld, J. D., Henderson, J. I., Kolagunta, V. R., Kubiak, C. P., Mahoney, W. J. and Osifchin, R. G.**, 1996, Self-assembly of a two-dimensional superlattice of molecularly linked metal clusters, *Science*, **273**, 1690-1693.

[90] **Ono, K., Okuda, R., Ishii, Y., Kamimura, S. and Oshima, M.**, 2003, Synthesis of ferromagnetic mn-pt nanoparticles from organometallic precursors, *Journal of Physical Chemistry B*, **107**, 1941-1942.

[91] **Hodak, J. H., Henglein, A., Giersig, M. and Hartland, G. V.**, 2000, Laser-ınduced ınter-diffusion in auag core-shell nanoparticles, *Journal of Physical Chemistry B*, **104**, 11708-11718.

[92] **Doering, W. E. and Nie, S.,** 2002, Single-molecule and single-nanoparticle: Examining the roles of surface active sites and chemical enhancement, *Journal of Physical Chemistry B*, **106**, 311-317.

[93] **Haes, A. J. and Van Duyne, R. P.**, 2002, A nanoscale optical biosensor: sensitivity and selectivity of an approach based on the localized surface plasmon resonance spectroscopy of triangular silver nanoparticles, *Journal of the American Chemical Society*, **124**, 10596.

[94] **Huang, X., Qian, W. and El-Sayed, M.A.,** 2006, Cancer cell imaging and photothermal therapy in the near-infrared region by using gold nanorods, *Journal of the American Chemical Society*, **128**, 2115-2120.

[95] **Mirkin, C. A., Letsinger, R. L., Mucic, R. C. and Storhoff, J. J.**, 1996, A DNA-based method for rationally assembling nanoparticles into macroscopic materials, *Nature*, **382**, 607-609.

[96] **Liu, J. and Lu, Y.**, 2004, colorimetric biosensors based on dnazyme-assembled gold nanoparticles, *Journal of Fluorescence*, **14**, 343-354.

[97] **Fan, F. R. F. and Bard, A. J.**, 2002, Chemical, electrochemical, gravimetric, and microscopic studies on antimicrobial silver films, *Journal of Physical Chemistry B*, **106**, 279-287.

[98] **Tsai, S. H., Liu, Y. H., Wu, P. L. and Yeh, C. S.**, 2003, Preparation of Au-Ag-Pd trimetallic nanoparticles and their application as catalysts, *Journal of Materials Chemistry*, **13**, 978.

[99] **Stanton, J. M.**, 1959, Isocyanate-modified drying oils, *Journal of the American Oil Chemists Society*, **36**, 503-507.

[100] **Vogel, A. I.**, 1970, *A Text Book of Practical Organic Chemistry Including Qualitative Organic Analysis*, Third edition, Longman, London, 689-690.

[101] **Cocks, L. V. and Rede, V.C.**, 1966, *Laboratary handbook for oil and fat analysis,* Academic press, London and New York, 80-126.

[102] **DIN 53152**, 1959, Deutsche normen, deutscher normenausschuss (DNA), October 1959.

[103] **ASTM D 1647-89**, 1991, Standart test methods for resistance of dried films varnishes to water and alkali, *Annual book of ASTM standarts,* **6**, 236-237.

[104] **ASTM D 3359-90**, 1991, Standart test methods for measuring adhesion by tape test, test method B, *Annual book of ASTM standarts,* **6**, 511-514

[105] **Lala, N. L., Ramaseshan, R., Li, B. J., Sundarrajan, S., Barhate, R. S., Liu, Y. J. and Ramakrishna, S.**, 2007, Fabrication of nanofibers with antimicrobial functionality used as filters: protection against bacterial contaminants, *Biotechnology and Bioengineering*, **97**, 1357-1365.

[106] **Hong, K. H., Park, J. L., Sul, I. H., Youk, J. H., and Kang, T. J.**, 2006, Preparation of antimicrobial poly(vinyl alcohol) nanofibers containing silver nanoparticles, *Journal of Polymer Science Part B-Polymer Physics*, **44**, 2468-2474.

[107] **Yu, H. J., Xu, X. Y., Chen, X. S., Lu, T. C., Zhang, P. B. and Jing, X. B.**, 2007, Preparation and antibacterial effects of pva-pvp hydrogels containing silver nanoparticles, *Journal of Applied Polymer Science*, **103**, 125-133.

[108] **Chou, W. L., Yu, D. G., and Yang, M. C.**, 2005, The preparation and characterization of silver-loading cellulose acetate hollow fiber membrane for water treatment, *Polymers for Advanced Technologies*, **16**, 600-607.

[109] **Jain, P. and Pradeep, T.**, 2005, Potential of silver nanoparticle-coated polyurethane foam as an antibacterial water filter, *Biotechnology and Bioengineering*, **90**, 59-63.

[110] **Gultekin, M., Beker, U., Guner, F. S., Erciyes, A. T. and Yagci, Y.**, 2000, Styrenation of castor oil and linseed oil by macromer method, *Macromolecular Materials and Engineering*, **283**, 15-20.

[111] **Erkal, F. S., Erciyes, A. T. and Yagci, Y.**, 1993, A new method for the styrenation of triglyceride oils for surface-coatings, *Journal of Coatings Technology*, **65**, 37-43.

[112] **Yagci, Y. and Schnabel, W.,** 1992, New aspects on the photoinitiated free-radical promoted cationic polymerization, *Makromolekulare Chemie-Macromolecular Symposia*, **60**, 133-143

[113] **Kabasakal, O. S., Guner, F. S., Arslan, A., Ergan, A., Erciyes, A. T. and Yagci, Y.**, 1996, Use of castor oil in the preparation of various oil-based binders, *Journal of Coatings Technology*, **68**, 57-62.

[114] **Kabasakal, O. S., Guner, F. S., Erciyes, A. T. and Yagci, Y.**, 1995, Styrenation of oil based on secondary esters of castor-oil, *Journal of Coatings Technology*, **67**, 47-51

[115] **Guner, F. S., Usta, S., Erciyes, A. T. and Yagci, Y.**, 2000, Styrenation of triglyceride oils by macromonomer technique, *Journal of Coatings Technology*, **72**, 107-110.

[116] **Guner, F. S., Yagci, Y. and Erciyes, A. T.**, 2006, Polymers from triglyceride oils, *Progress in Polymer Science*, **31**, 633-670.

[117] **Sooklal, K., Hanus, L. H., Ploehn, H. J. and Murphy, C. J.,** 1998, A blue-emitting Cds/dendrimer nanocomposite, *Advanced Materials*, **10**, 1083-1087.

[118] **Qi, L. M., Colfen, H. and Antonietti, M.**, 2001, Synthesis and characterization of Cds nanoparticles stabilized by double-hydrophilic block copolymers, *Nano Letters*, **1**, 61-65.

[119] **Zhao, H. Y., Douglas, E. P., Harrison, B. S., and Schanze, K. S.**, 2001, Preparation of Cds nanoparticles in salt-ınduced block copolymer micelles*, Langmuir*, **17**, 8428-8433.

CURRICULUM VITA

Candidate's full name: Osman EKSİK

Place and date of birth: Istanbul, 1973

Permanent Address: Rauf Paşa Hanı Sokak, Çamlıca Konakları 7/2
34660 Acıbadem Istanbul

Universities and Colleges attended: Istanbul Technical University

Publications:

•**O. Eksik,** A. T. Erciyes, Y. Yagci, "In situ synthesis of oil based polymer composites containing silver nanaoparticles", *J. Macromol. Sci. Part A-Pure and Appl.Chem,*. 45, 698-704, **(2008)**

•**O. Eksik,** M. A. Tasdelen, A. T. Erciyes, Y. Yagci, "In situ synthesis of oil based polymer/silver nanocomposites by photoinduced electron transfer and free radical polymerization processes", Composite Interfaces *in submitted*